Thesis

Effects of recombinant leptin on immortalized human chondrocyte cell lines C28/I2 and T/C-28a2

- An experimental analysis

Submitted by

Florian Halbartschlager

For the degree of

Doctor medicinae universiae

(Dr. med. univ.)

At the

Medical University of Graz (AUT)

Performed at

Department of Orthopedics and Orthopedic Surgery

Supervised by

Priv.-Doz.in Mag.a rer.nat. Dr.in scient.med. Birgit Lohberger

Priv.-Doz.in Mag.a Dr.in rer.nat. Bibiane Steinecker-Frohnwieser

Institute of Biophysics

Graz, December 5, 2016

Declaration

I hereby declare that I have authored this thesis independently, that I have not used other than the declared sources / resources, and that I have explicitly marked all material which has been quoted either literally or by content from the used sources.

Graz, December 5, 2016 *Florian Halbartschlager eh*

Acknowledgement

First of all, I would like to thank my supervisor Dr. Birgit Lohberger, for the opportunity to write this thesis. I am very grateful for her support, helpful advices and her engagement during the whole time of the study. Special thanks goes to Heike Kaltenegger and Nicole Stündl for their patience and assistance during my first steps into laboratory work and throughout the study.

My greatest appreciation goes to my parents Christa and Johann who supported me in every possible way to have worriless and unforgettable student days.

Abstract

Background: Osteoarthritis (OA) is a degenerative joint disease and one of the most frequent causes of musculoskeletal disability and pain around the world. Obesity is an important risk factor, not only the weight-related joint destruction, but also the highly inflammatory state in the joints of obese individuals, which leads to an imbalance of anabolic and catabolic factors in articular cartilage. Increasing evidence support the idea of leptin, an adipocytokine, being the non-mechanical link between morbid obesity, joint integrity and OA.

Objectives: To investigate the effect of recombinant leptin on the cell proliferation and the expression of anabolic and catabolic components in the immortalized human chondrocyte cell lines C28/I2 and T/C-28a2.

Methods: Characterization of the C28/I2 and T/C-28a2 cell lines was performed via STR-analyses. Additionally a specific vimentin-DAPI immunofluorescence imaging was performed to confirm the mesenchymal origin of the cells. The human chondrocyte cell lines were treated with recombinant leptin and their cell viability and growth behavior was examined by using a MTS- cell viability assay and a xCELLigence RD device system. Furthermore the gene expression levels of anabolic and catabolic cartilage-specific components (MMP-1, MMP-3, MMP-9, MMP-13, collagen 1A1 and collagen 2A1) were investigated by real-time PCR in order to gain information about chondrocyte responsiveness to leptin after a time period of 48 h. The effects of leptin on the expression of collagen and sGAG on protein levels were investigated by colorimetric measurements.

Results: The growth behavior was recorded for 77 h and indicated that C28/I2 as well as T/C-28a2 need foetal bovine serum (FBS) essentially to grow regularly. Moreover the MTS tests showed, that the leptin treatment [0.001 µg/ml; 0.01 µg/ml; 0.1 µg/ml; 0.5 µg/ml; 1.0 µg/ml] for 24 h and 48 h has no significant negative effect on the cell viability of the cell lines. In addition the real-time PCR results showed a significant decrease of the MMP-1 and MMP-13 gene expression levels in T/C-28a2 cells when treated with 0.2 µg/ml leptin. Collagen 1A1 has a significant decreased expression in C28/I2 cells after the treatment with leptin [0.2 µg/ml]. Whereas collagen 2A1 was detected to have a decreasing tendency in both cell lines after the treatment with leptin [0.2 µg/ml and 0.5 µg/ml].

Additionally protein levels of collagen were surveyed to be slightly up regulated in the leptin + IL-1β setup (C28/I2), whereas C28/I2 cells without IL-1β showed a low decrease of collagen. No significant changes in the protein expression of sulfated glycosaminoglycan (sGAG) in C28/I2, but a declining leptin + IL-1β induced tendency of sGAG were analyzed.

Discussion: Our data provide interesting insights in the OA pathogenesis and the relationship between OA and obesity.
Further *in vitro* studies are required to elucidate the complex mechanisms of leptin and to find new targets in the therapy of obesity induced OA.

Zusammenfassung

Hintergrund: Osteoarthritis ist eine degenerative Gelenkserkrankung, welche weltweit eine der häufigsten Ursachen für muskuloskeletale Beeinträchtigungen und Schmerzzustände ist. Ein wichtiger Risikofaktor stellt hierbei Adipositas dar, welcher nicht nur im offensichtlichen Verschleiß der Gelenke durch das erhöhte Körpergewicht, sondern überdies im ausgeprägten pro-inflammatorischen Zustand in den Gelenkshöhlen von Übergewichtigen begründet ist. Dieser Zustand fördert das Ungleichgewicht von aufbauenden und abbauenden Faktoren in den Gelenksknorpeln. Es gibt immer mehr Belege dafür, dass Leptin – ein Adipozytokin – die nicht-mechanische Verbindung zwischen Adipositas, Gelenksintaktheit und Osteoarthritis darstellt.

Zielsetzung: Untersuchung des Einflusses von rekombinantem Leptin auf das Zellwachstum und die Expression von aufbauenden und abbauenden Faktoren der menschlichen Chondrozytenzelllinien C28/I2 und T/C-28a2.

Methoden: Die Zelllinien C28/I2 und T/C-28a2 wurden mittels STR-Analyse charakterisiert. Im weiteren Verlauf wurde eine spezifische Vimentin-DAPI Immunfluoreszenzfärbung durchgeführt, um den mesenchymalen Ursprung der Zellen zu verifizieren. Die Lebensfähigkeit und das Wachstumsverhalten der humanen Knorpelzellen nach der Behandlung mit rekombinantem Leptin wurde mittels MTS- Cell Viability Test und xCELLigence RD Device System untersucht. Zusätzlich wurde die Genexpression von anabolen und katabolen Komponenten (MMP-1, MMP-3, MMP-9, MMP-13, Collagen Typ 1A1 and Collagen Typ 2A1) via Real-Time PCR ermittelt, um Information über die Antwort der Chondrozyten auf Leptin nach 48 Stunden zu erhalten. Biochemische Testverfahren wurden benutzt, um Informationen über die Wirkung von Leptin auf die Expression von Collagen und sGAG auf Proteinebene zu erlangen.

Ergebnisse: Das Wachstumsverhalten wurde über einen Zeitraum von 77 Stunden analysiert und hat gezeigt, dass die Zugabe von FBS essentiell für das reguläre Wachstum sowohl von C28/I2 als auch T/C-28a2 Zelllinien ist. Mit Hilfe eines MTS Test konnte überdies gezeigt werden, dass eine Leptin Behandlung [0,001 µg/ml; 0,01 µg/ml; 0,1 µg/ml; 0,5 µg/ml; 1,0µg/ml] über 24 und 48 Stunden keinen signifikanten negativen Einfluss auf die Lebensfähigkeit der Zelllinien hat.

Weiters zeigten die Ergebnisse der Real-Time PCR für die T/C-28a2 Zelllinie, welche mit Leptin [0,2 µg/ml] behandelt wurde, eine signifikante Abnahme der MMP-1 und MMP-13 Genexpressionslevel. Zusätzlich konnte eine signifikante Abnahme der Genexpression von Collagen Typ 1A1 bei den mit Leptin [0,2 µg/ml] behandelten C28/I2 Zellen festgestellt werden. Für Collagen Typ 2 zeigte sich hingegen eine abnehmende Tendenz der Genexpression bei beiden Zelllinen nach der Inkubation mit Leptin [0,2 µg/ml and 0,5 µg/ml]. Abschließend ermittelten wir die Collagenexpression auf Proteinebene. Hierbei zeigte sich für die C28/I2 Zellen eine leichte Zunahme der Proteinmenge in dem Leptin plus IL-1β Versuch, wohingegen dieser Effekt ohne IL-1β nicht beobachtet werden konnte und es zu einer geringfügigen Abnahme der Proteinmengen kam. In der Expressionsanalyse der Proteinmenge von sGAG in C28/I2 Zellen zeigten sich keine signifikanten Änderungen, wohl aber war eine abnehmende Tendenz von sGAG in dem Leptin und IL-1β kombiniertem Versuchsaufbau zu erkennen.

Diskussion: Unsere Daten bringen interessante Erkenntnisse über die Pathogenese von OA und beleuchten den Zusammenhang zwischen OA und Adipositas.
Es werden weitere *in vitro* Untersuchungen nötig sein, um die komplexen Mechanismen von Leptin näher auszuführen und um neue Therapieansätze bei der Adipositas induzierten OA zu entwickeln.

Contents

Abbreviation

A

ADAMTS	a desintegrin and metalloproteinase with thrombospondin motifs
ACL	anterior cruciate ligament
ACTB	beta- actin

C

Ca^{2+}	calcium ions
$CaCl_2$	calcium chloride
CCM	cell culture medium
CI	cell index
CO_2	carbon dioxide
COL1A1	collagen 1A1
COL2A1	collagen 2A1
COX-2	cyclooxygenase-2
Cy-2	cyanin-2

D

DA	dalton
kDA	kilodalton
DAPI	4´, 6-diamidino-2-phenylindole
Db	diabetes
DNA	deoxyribonucleic acid
dsDNA	double-stranded deoxyribonucleic acid
ssDNA	single-stranded deoxyribonucleic acid

E

EDTA	ethylenediaminetetraacetic acid
ECM	extracellular matrix

F

FBS	foetal bovine serum
FFA	free fatty acids
FGF	fibroblast growth factor
FU	fluorescence unit
FV	forward

G

sGAG	sulfated glycosaminoglycan
GAPDH	glyceraldehyde 3-phosphate dehydrogenase
GDF5	growth differentiation factor 5
GER	Germany

H

H	hours
HDL	high-density lipoprotein
HDL-c	high-density lipoprotein cholesterol
HPRT	hypoxanthine phosphoribosyl-transferase

I

INF-γ interferon-γ

IL Interleukin

J

JAK/STAT janus kinase/signal transducer and activator of transcription

K

KL Kellgren and Lawrence

L

LDL-c low-density lipoprotein cholesterol

M

MAPK mitogen-activated protein kinase

β-ME mercaptoethanol

$MgCl_2$ magnesium chloride

MIQE minimum information for publication of qRT-PCR experiments

MMLV moloney murine leukemia virus

MMP Metalloproteinase

MRI Magnetic Resonance Imaging

MTS (3-(4,5-dimethylthiazol-2-yl)-5(3carboxymethoxyphenyl) -2-(4-sulfophenyl)-2H-tetrazolium, inner salt

N

NaHO sodium hydroxide

NO nitric oxide

iNOS inducible nitric oxide synthase

dNTPS deoxynucleotide triphosphates

NT nucleotide

O

OA Osteoathritis

Ob obese

OBR obese receptor

Ox-LDL oxidized low-density lipoprotein

P

PES phenazine ethosulfate

PGE2 prostaglandin E2

R

RF risk factors

RIN RNA integrity number

RNA ribonucleic acid

siRNA small interference RNA

ROS reactive oxygen species

RPM rounds per minute

RT-qPCR real-time quantitative polymerase chain reaction

Rt room temperature

RV reverse

S

SD	standard deviation
SF	synovial fluid
SOCS	suppressor of cytokine signaling

T

TG	triglycerides
TGF	transforming growth factor
TNF-α	tumor-necrosis factor-α
TRIS HCL	Tris(hydroxymethyl) aminomethane hydrochloride

U

UK	United Kingdom

V

VCAM	vascular cell adhesion molecule

W

WHO	World Health Organisation
WTD	western type diet

Y

YLD	years lived with disability

Index of Figures

Index of Tables

1 Introduction

1.1 Defining Osteoarthritis

Osteoarthritis (OA) represents a degenerative joint disorder and is characterized by destructions leading to a progressive loss in articular cartilage, hypertrophy of the bone and joint capsule thickening with subsequent pain symptoms, limitation of movement and a variable state of inflammation (1)(2)(3).

With the need of standardization and practicability, radiography is the most common clinical standard defining OA. The presence and severity of OA are scored by the Kellgren and Lawrence (KL) grading system. The severity is measured on a scale from 0 to 4, whereby >2 define radiographic OA by checking these five radiological features: osteophytes, perarticular ossicles, narrowing of joint cartilage, small pseudocystic areas and altered shapes of bone ends (4). The KL grading system is used for hand, hip and knee joints. In addition tibiofemoral OA can be assessed without adjusted x-ray views, whereas patellofemoral OA can only be assessed with adjusted views (4).

In terms of Magnetic Resonance Imaging (MRI) there is no validated definition for OA (5). However there are well-described MRI lesions: bone marrow lesions, cartilage lesions, subchondral bone attrition, synovitis, osteophytes and effusions (Figure 1). At least one MRI lesion can be found in knees of middle-aged adults without radiographic evidence (KL 0) independent of clinical symptoms such as pain (6)(7)(8).

Withal OA can be diagnosed in various ways, such as clinically, pathologically or radiographically. Which way to use best, depends on the medical questioning, the available clinical setting and the operator.

Figure 1: MRI demonstrating knee OA features
(**A-C**) Sagittal Inversion Recovery MRI, **A=** Reactive Synovitis (**arrow**); **B=** Subchondral Cyst Formation (**arrow**); **C=** Bone Marrow Edema (**arrows**); (**D-F**) Coronal Fast Spin-echo MRI, **D=** Partial thickness Cartilage Wear (**arrow**); **E+F=** Full thickness Cartilage Wear (**thin arrows**), Subchondral Sclerosis (**arrowhead**), and Marginal Osteophyte Formation (**double tailed arrow**).
Images courtesy of Drs. Hollis Potter and Catherine Hayter, Hospital for Special Surgery, New York, NY.
Source adapted from: (9).

1.2 Epidemiology of OA

Based on the aging population, increasing obesity and the lack of activity, OA is the fastest increasing major health condition. The estimated number of people worldwide living with knee OA is 250,785 million (10).

Disabilities related to musculoskeletal disorders are estimated to have increased by 45% from 1990 to 2010 (10). Measured by years lived with disability (YLD) OA is ranked second causing disability (OA: 21.3%, mental and behavioral disorders: 22.7%) (10).

Whereby 80% of the people with OA have limitations and already 25% are not able to perform their major daily activities of life (10,11).

The continuous increase of OA prevalence is closely linked to a significant socioeconomic burden in developed countries. This requires an adjusted and well planned use of health resources in the future (12).

1.3 Risk Factors

Risk factors (RF) for OA can be split into person-level RF and joint-level RF.

1.3.1 Person-level risk factors

OA is more likely with increased age, especially >50 years and additionally female sex compared to male sex is an import RF. Females incline to a more severe OA, especially in after menopausal age. Differences between female and male also occurred with the OA related joint sites (13)(14).

There are many sources, indicating a strong linkage between genetics and OA. Large family and twin studies approved a significant coherence of genetic factors (39-70%). Noteworthy, genetic factors related to OA are specific to individual joint sites and cannot be explained by one genetic mechanism (15).
Many genes were discovered to matter in the pathological pathways of OA and were assumed to be strong risk factors but also targets for new therapeutic approaches, e.g. genes for Vitamin D receptors, insulin-like growth factor 1 (16), growth differentiation factor 5 (17) and collagen 2A1 (18). By now, three loci were discovered related to OA at the genome-wide significance level: chromosome 7q22 (19), MCFL2 (20) and GDF5, codifying growth differentiation factor 5 (a bone morphogenetic protein expressed in skeletal and articular structures) (13)(21).

1.3.2 Joint-level risk factors

The repetitive use of joints is associated with an increasing risk for OA. Studies have proved that there is a doubled risk for knee OA in individuals whose occupations including squatting or kneeling compared to occupation without physical activity. Especially jobs required heavy lifting and prolonged standing are associated with OA. There is also evidence that jobs requiring increased manual dexterity are associated with OA events in the hand joints (22)(23).

Sport and physical activity with habitual intensity is discussed to be protective to the joints, due to the strengthening of the periarticular muscles helping to stabilize the joints. Studies with elite-level athletes have come to controversial results, due to biases which could not

be ruled out. Elite-level athletes have increasing risk of developing OA as they get older compared to an age-matched, non-elite cohort. But it is not clarified if this occurs due to the more intense and highly repetitive joint use associated with sports like tennis, squash and team sports or due to the more frequently presence of injuries (24).

The integrity of the joints is influenced by many factors. Injuries resulting in a tear of the anterior cruciate ligament (ACL) often linked to direct cartilage damage. The most notable injury affecting the joint integrity and causing OA in the knee, is the tear of the menisici (25).
Furthermore anatomical morphology differing from physiological advantageous shape is a risk factor in the development of OA. Due to the biomechanical load, now affecting parts of the joints, which are not able to carry these loads (e.g. a mild acetabular dysplasia is associated with hip OA) (26).
All these risk factors allow the differentiation of OA into several phenotypes, i.e., post-traumatic, aging-related, genetic and symptomatic. Metabolic OA is a newly defined phenotype and discusses OA in association with the metabolic syndrome and obesity (27).

Osteoarthritis is a complex and multifactorial disease, until now several risk factors are identified. Some RF are modifiable and preventable and efforts minimizing these RF can help to reduce the impact of OA.

1.4 Obesity and OA

The World Health Organization (WHO) defines obesity by a Body Mass Index >30kg/m^2 (28). Obesity is an important risk factor for weight and non-weight bearing joints. For weight-bearing joints obtains, the increased forces are a direct stress to the cartilage and the subchondral bone. In chondrocytes, the only cells present in cartilage, this abnormal load induces the production of catabolic tissue remodeling enzymes like matrix metalloproteinases (MMP). The up regulation of MMP-1, -3 and -9 accompanied with proteoglycan loss and cartilage damage is caused by high cyclic tensile load. Similar effects are observed for load-injured articular cartilage explants: up regulation of MMP-3 levels and proteoglycan loss and collagen damage. These processes can affect the joint directly. But the heavy loading can also change the inflammatory state in chondrocytes.

Chondrocytes exposed to high loadings have an increasing expression of pro-inflammatory cytokines: IL-1β, tumor-necrosis factor-α (TNF-α), cyclo-oxygenase-2 (COX-2) and prostaglandin E2 (PGE2) (29–32).

Whereas once knee-OA was considered a "wear-and-tear" condition, it is now recognized that OA also exists in the highly metabolic and inflammatory environment of adiposity (33). Recently, a positive association between overweight or morbid obesity and osteoarthritis was observed not only for knee joints but also for non-weight bearing joints, such as finger joints (34). Metabolic triggered inflammation (referred to as meta-inflammation) is based on abnormalities in the body composition, cytokines, complements, and adipokines (35).

An abnormal lipid profile, labeled as dyslipidemia, is a typical characteristic of obesity. Due to obesity induced dyslipidemia, high plasma levels of triglycerides (TGs), low levels of high-density lipoprotein cholesterol (HDL-c), small increased levels of low-density lipoprotein cholesterol (LDL-c), increased levels of free fatty acids (FFAs) and an impaired high-density lipoprotein (HDL) function are observed. Multiple studies have shown, that lipid metabolism can play a role in OA (36,37) (Figure 2). By stimulating the toll-like receptor 2/4 FFAs are able to activate macrophages (38). Macrophages produce pro-inflammatory mediators causing a severe adipose tissue and joint inflammation leading to a condition supporting OA. It was demonstrated that low HDL levels with additional factors e.g. western type diet (WTD= 42% energy from fat) can push the cartilage homeostasis in an OA supporting direction (39).

Furthermore reactive oxygen species (ROS) can oxidize LDL leading to oxidized LDL (ox-LDL), which induces a cascade of pro-inflammatory mediators leading to an increase of the pro-inflammatory state (40). As obesity develops, adipocytes release active components like the adipokines leptin, visfatin, adiponectin, chemerin, lipocalin-2 and resistin as well as interleukin IL-6, IL-1 and tumor-necrosis factor-α (TNF-α) which lead to metabolic dysfunction in OA patients and disruption of cartilage homeostasis (Figure 2).

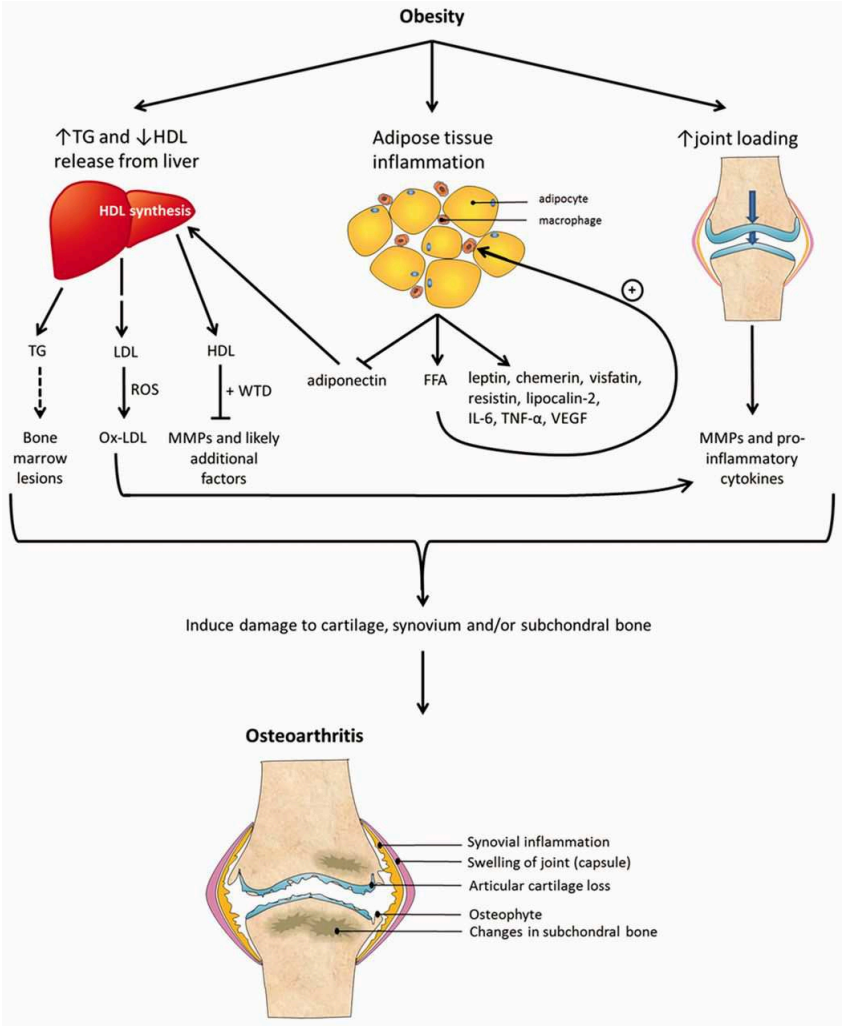

Figure 2. Factors associated with obesity and OA
Dyslipidaemia, adipose tissue inflammation and increased joint loads are associated with obesity. This condition is characterized by low release of functional high-density lipoprotein (HDL) and high systemic levels of triglycerides (TGs), free fatty acids (FFAs), oxidized low-density lipoprotein (ox-LDL), adipokines and pro-inflammatory cytokines. These factors cause a high inflammatory setting, which can result in a lack of joint and bone integrity and eventually OA. Source adapted from: (33).

1.5 Leptin

1.5.1 Leptin and leptin receptors

Leptin, mainly produced by the white adipose tissue (but also in chondrocytes), is a 16 kDa non-glycosylated protein, a product of the obese (ob) gene. It was originally described by Zhang et al. in 1994 as regulator for food intake and energy expenditure (41). Leptin signals by binding to the leptin receptors (OBR), these receptors are encoded through the diabetes (db) gene and are members of the class I cytokine receptor superfamily.

At least five alternatively sliced receptor isoforms, which differ by the length of their cytoplasmic domains, were detected with reduced transduction capabilities. Therefore only the long isoform (OB-Rb) with its full intracellular domain is able to transduce the leptin-binding signaling in an effective way via e.g. the activation of the Janus kinase/signal transducer and activator of transcription (JAK/STAT) signal transduction pathway. Besides the JAK/STAT pathway, it is possible to produce a signaling through alternative pathways e.g. the mitogen-activated protein kinase (MAPK) pathway (42–45).

1.5.2 Leptin associated with OA

Plasma leptin levels, as well as synovial fluid (SF) levels correlate positively with the Body Mass Index (46)(47). A recent study showed a positively correlation between knee OA and plasma leptin levels in middle-aged women (48). Interestingly the SF leptin level exceeds the leptin levels measured in plasma by 3 to 11 times (46). This suggests that local leptin levels have a bigger impact in the bone and cartilage homeostasis than systemic leptin levels. Leptin is suggested to be a potential quantitative biomarker for OA due to the fact, that SF leptin levels are associated with the radiographic severity of OA as well as with MMP-1 and MMP-3 levels. A connection between intra-articular concentrations of several adipokines and severity of preoperative OA pain was determined, whereas SF leptin levels played a key role in the pathogenesis of hip and knee OA (49)(50)(51).
A study investigating the correlations of OA, obesity and leptin in mice detected that obesity itself cannot induce systemic inflammation and knee OA. Obesity without the signaling of leptin is not impactful enough developing obesity-related OA (52). This is important information regarding the coherence between leptin, obesity and OA.

All these studies support the idea, that leptin is the non-mechanical link between obesity, joint integrity and OA.

1.5.3 Leptin effects

In OA joints leptin causes a mismatch of anabolic and catabolic mediators leading to the loss of integrity in the affected joints by remodeling and destroying articular cartilage. In articular tissues that undergo various structural and biochemical changes during OA, leptin is strongly up regulated when compared with healthy tissues (47)(53). Furthermore leptin

is a regulator of chondrocyte functions and is able to produce an inflammatory and destructive condition in joints (Figure 3).
This condition develops through pro-inflammatory mediators, which are enhanced in OA chondrocytes. Nitric oxide (NO) promotes apoptosis, chondrocyte phenotype loss and MMP activation. Inducible nitric oxide synthase (iNOS) in synergy with interferon γ (INFγ) both induced by leptin can directly damage articular cartilage (54). Furthermore leptin synergizes with interleukin-1β (IL-1β) to boost the production of iNOS, prostaglandin E2 (PGE2) and cyclooxygenase-2 (COX-2) in human chondrocytes (55). Additionally leptin is able to secrete higher levels of pro-inflammatory cytokines such as IL-1β, IL-6, IL-8 which are mainly responsible for cartilage remodeling (56). Further Conde et al. treated human and murine chondrocytes with leptin and described an increased secretion of vascular cell adhesion molecule (VCAM-1) (57).

Bao et al. demonstrated that the *in vivo* injection of leptin into rat knee joints enhance the production of extracellular cartilage-degrading MMP-1, MMP-3, MMP-9, MMP-13 which benefits catabolic effects in OA cartilage (58). Interestingly, a decreased MMP-13 expression was detected in cartilage of OA patients with downregulation of leptin with small interference RNA (siRNA) (59). The treatment with leptin also leads to an increased transcriptional expression of a disintegrin and metalloproteinase with thrombospondin motifs (ADAMTS-4 and ADAMTS-5) two important aggrecanases. All these results and additionally the decrease of anabolic factors like basic fibroblast growth factors (FGF) confirming the prominent catabolic effect of leptin in cartilage homeostasis of OA joints (58).

In contrast to the catabolic effects of leptin, another study showed an increase of chondrocyte proliferation and enhanced synthesis of proteoglycans and collagen under the influence of leptin (60). In addition, it was demonstrated that intra-articular leptin injection can induce the production of the insulin-like growth factor 1 (IGF-1) and the transforming growth factor β (TGF-β) (47). This may occur to the fact, that leptin itself has an anabolic effect or that the adipokine triggers compensatory anabolic responses.

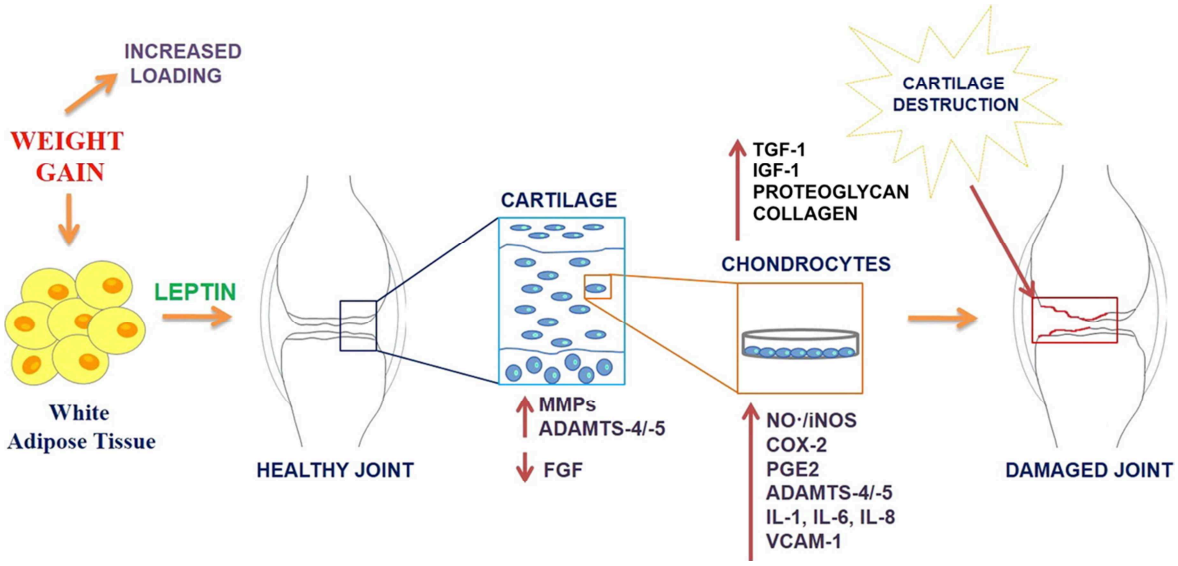

Figure 3. Schematic overview of Leptin effects
Source adapted from: (61).

1.6 Study objectives

All these outcomes support the idea of leptin being the non-mechanical link between obesity, joint integrity and OA. Despite all, there is no data about the influence of recombinant leptin on immortalized human chondrocyte cell lines C28/I2 and T/C-28a2.

Therefore this study provides information about:

- **Characterization of the chondrocyte** cell lines was performed using short tandem repeat analysis via Powerplex16 System Kit (Promega) in combination with a vimentin-DAPI immunofluorescence imaging to confirm the mesenchymal origin.
- **Cell viability** under influence of leptin was assessed with a MTS- cell viability assay (Promega).
- **Cell growth behavior** in presence and absence of foetal bovine serum as well as the influence of different quantities of seeded cells was analyzed by an xCELLingence RD device system (ACEA Biosciences).
- Changes in the **extracellular matrix composition** after leptin treatment were detected by using a RT-qPCR in order to gain information especially about MMPs and collagen. Newly synthesized collagen was also determined throughout a Sircol™ photometric assay (BioColor). Conclusively the quantity of newly secreted sulfated Glycosaminoglycan was ascertained using a Blyscan™ colorimetric assay (BioColor).

2 Methods

2.1 Cell lines

The C28/I2 and T/C-28a2 chondrocyte cell lines were kindly provided by Prof. M.B. Goldring (Harvard Institute of Medicine, Boston, MA). The C28/I2 chondrocyte cell line was treated with Interleukin-1β (IL-1β) [10ng/ml] to generate a pro-inflammatory osteoarthritis model in comparison to the T/C-28a cell line. Both cell lines were verified by PCR-based short tandem repeat analysis using a Powerplex16 System Kit (Promega, Mannheim, Germany).

Short tandem repeats also referred to as microsatellite, are small repetitive parts of DNA, which have an extremely high variety in the human population, due to their high mutation rate. The length of short tandem repeats varies usually from 2 to 5 base pairs and are repeated up to 5 to 50 times (62). As a consequence there is an exceptionally high chance that two individuals differ by their constellations of microsatellites. Because of this polymorphic character, short tandem repeats are used as state-of-the-art analysis for e.g. forensic DNA profiling or like in this case for genetic linkage analysis (63).

2.1.1 Cell Culture Conditions

The C28/I2 and T/C-28a2 chondrocyte cell lines were cultured in Dulbecco´s modified Eagle medium with high glucose DMEM-HG (Gibco®, life technologies™, Carlsbad, U.S.A.) The cell culture medium was complemented with amphotericin B [0.1%] (PAA Laboratory, Pasching, Austria), l-glutamine [1.0%] (Gibco®, life technologies™), ascorbic acid [0.05mg/ml] (Sigma Aldrich, St. Louis, U.S.A.), penicillin streptomycin [1%] (Gibco®, life technologies™), and foetal bovine serum [10%], FBS (Gibco®, life technologies™). The medium was changed every three days.
Cells were stored and cultured at humidified atmosphere at 37°C with CO_2 [5%] and were sub-cultured with Accutase® (Innovative Cell Technologies, San Diego, U.S.A.), once reached confluence as judged by microscopy. Cell cultures were checked on regular basis for contaminations.

2.1.2 Vimentin-DAPI Immunofluorescence

A vimentin-DAPI immunofluorescence analysis was performed to confirm the mesenchymal origin of the C28/I2 and T/C-28a2 cell lines. Vimentin is an intermediate filament protein with a molecular weight of 57 kDa. The proteins form parts of the cytoskeleton structure of vertebrate cells. There are 5 classes of intermediate filament proteins, whereby vimentin belongs to class III showing a high specificity towards cells with a mesenchymal origin.

The cells were first labeled with a monoclonal anti-vimentin antibody (Dako, Santa Clara, U.S.A.) and in a next step labeled with a second antibody, a cyanin-2 (cy-2) conjugated goat anti-mouse antibody (Jackson ImmunoResearch, West Grove, U.S.A.). In this cy-2 serves as fluorescence dye which links to the first antibody. This emerged complex can be visualized with a fluorescence microscope. For a better orientation concerning the imaging and analysis, the nuclei were counterstained with 4´, 6-diamidino-2-phenylindole (DAPI) which binds to DNA rich regions especially nuclei.

2.1.2.1 Protocol

At first, the vimentin antibody [156 mg/L] (Dako) was diluted [1:100; 1:200] with phosphate-buffered saline 1x (PBS; Gibco®, life technologies™, Carlsbad, U.S.A.) containing 1% bovine serum albumin (BSA) and Triton™ X-100 (Sigma Aldrich). The second antibody, the cy-2 conjugated goat anti-mouse antibody [1,5 mg/ml] (Jackson ImmunoResearch) was prepared in a solution at a ratio of 1:100 using the same antibody diluent.

The C28/I2 and T/C-28a2 cells were plated into chamber slides with 2500 cells/well. After incubation, the cells were rinsed with PBS 1x (Gibco) and dried for 1 hour at room temperature (rt) followed by an overnight storage at -20°C.
In a next step the chondrocytes were fixed using paraformaldehyde [4%] (pFA) for 10 minutes. Afterwards fixed chondrocytes were washed with PBS 1x (Gibco). Afterwards the cells were blocked with UltraVision ProteinBlock (Thermo Fisher Scientific) for 5 minutes (rt) to reduce unspecific protein bindings for a better imaging quality with less background.

Now the diluent containing the first antibody, the vimentin antibody (Dako) was added to each well (200 µl) and incubated for 30 minutes (rt).

After 30 minutes of incubation and washing steps with PBS 1x (3x5min), the cy-2 conjugated goat anti-mouse antibody (Jackson ImmunoResearch) was added (200 µl/well) and incubated for 30 minutes (rt) protected from light. A second round of washing steps with PBS 1x (3x5min) followed and subsequently the sections treated before were covered with a Vectashield Mounting Medium containing DAPI purchased from Vector Laboratories (Burlingame, U.S.A.) to counterstain the nuclei. Controls were performed as shown in Table 1.

Negative control	Antibody-diluent
Negative control	Antibody-diluent + mouse immunoglobulin G (IgG)
Negative control cells	MCF7 cells
Positive control cells	HeLa cells

Table 1. Controls for vimentin- DAPI immunofluorescence

The cells were stored in the dark and viewed with a Confocal LSM 510 META Fluorescence Microscope (Zeiss, Vienna, Austria). ZEN 2009 software (Zeiss) was used to take and process the images.

2.2 Leptin- processing and preparation

All trials were performed with recombinant human leptin (R&D Systems, Bio Techne, Wiesbaden-Nordenstadt, Germany). The recombinant human leptin used is an E.coli derived Val22-Cys167 with an N-terminal Met Protein. The adipokine was reconstituted at 1 mg/ml in sterile 20 mM Tris-HCl at pH 8.0. All aliquots were stored at -70°C as recommended.

2.3 xCelligence Real-time cell analysis

The xCelligence RD device System for Real-Time and Dynamic Monitoring of Cell Proliferation and Viability for Adherent Cells (ACEA Biosciences, Inc., San Diego, U.S.A.) uses a non-invasive impedance measurement to quantify adherent cell proliferation and viability in real time. T/C-28a2 and C28/I2 + IL-1β [10ng/ml] chondrocyte cell lines were seeded in 16-well micro plates (E-plates®, Roche Diagnostics, Rotkreuz, Switzerland)

containing microelectronic sensor arrays. The impedance generated when cells interacted with the gold biosensors (covering 70-80% of the wells) indicates the cell viability and also correlates with the number of seeded cells (Figure 4).

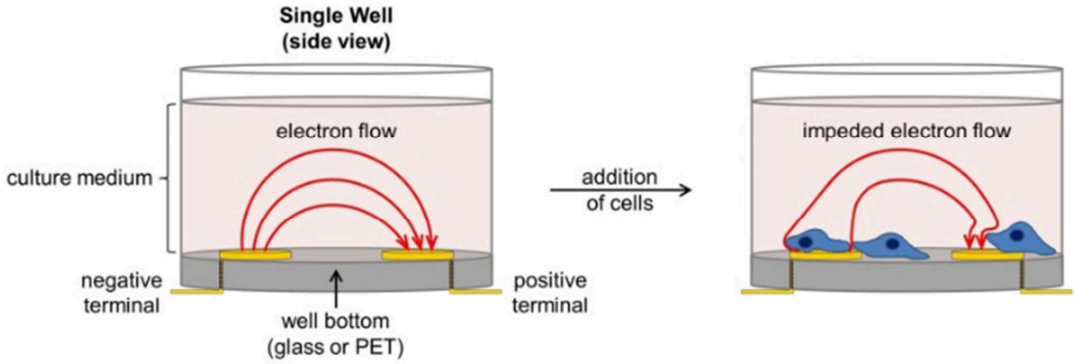

Figure 4. Overview of the xCELLigence impedance device
On the left side an empty well in side view with a regular electron flow from the negative to the positive terminal is shown. On the right side a well with seeded cells showing an impeded electron flow, which can be measured and analyzed. Source adapted from: (64).

The cell sensor impedance is converted to a unitless parameter called Cell Index (CI) (Figure 4). This unit is defined as impedance at time point n minus impedance in absence of cells divided by the nominal impedance value. Cells were monitored every 30 minutes for a time period of 77 hours. The assay was used to verify the role of FBS (Gibco®, life technologies™) for the specific chondrocyte cell lines as well as the optimal density of plated cells for further investigations.

2.3.1 Protocol

3000 cells/well and 5000 cells/well of T/C-28a2 and C28/I2 + IL-1β [10ng/ml] were seeded into a 16-well E-plates® (Roche Diagnostics) in 100µl of cell culture medium (CCM) according to Figure 5. Seeding was done approximately 24 hours prior to the treatment to ensure the cells were in the log growth phase. For the treatment 200 µl CCM containing FBS and 200 µl non-FBS containing CCM as a reference group was used according to Figure 5. Untreated cells were used as a control group.
Cell growth behavior was analyzed with the RTCA 1.2.1. Software (ACEA Biosciences Inc., San Diego, USA).

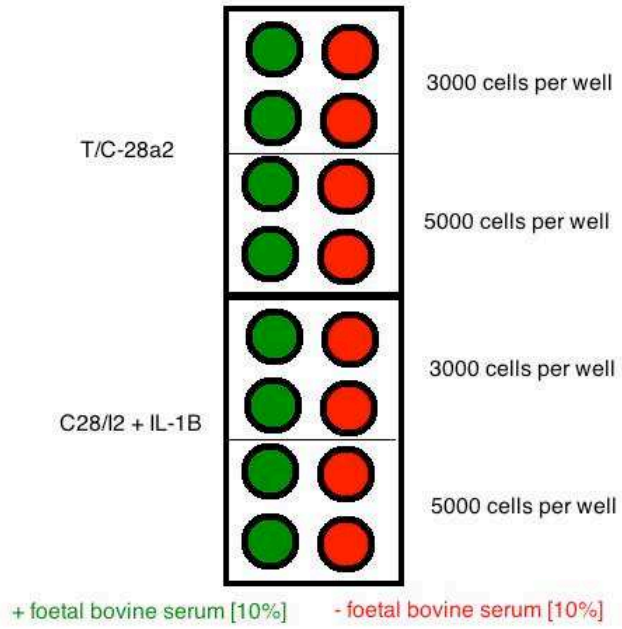

Figure 5. Seeding setup for Xcellingence real time cell analysis
Cells in green wells were seeded with FBS [10%], cells in red wells without FBS. Additionally T/C-28a2 and C28/I2+IL-1β were seeded with 3000 cells/well and 5000 cells/well. Source: FH

2.4 Cell viability assay

CellTiter 96®Aqueous One Solution Cell Proliferation Assay (Promega) was used to ascertain the cell viability of the C28/I2 and T/C-28a2 chondrocyte cell lines when treated with specific leptin concentrations based on a colorimetric method. The main contents of the CellTiter 96® Aqueous One Solution Reagent are a tetrazolium compound (3-(4,5-dimethylthiazol-2-yl)-5-(3-carboxymethoxyphenyl)-2-(4-sulfophenyl)-2H-tetrazolium, inner salt; MTS[(a)]) and an electron coupling reagent (phenazine ethosulfate; PES[(a)]).

The assay is based on the reaction by living cells bioreducing the MTS tetrazolium compound (Owen´s Reagent) into a colored formazan product (Figure 6), qualifying MTS to be used as a cell viability indicator. A 96-well plate reader is needed to measure the absorbance of the colored formazan product at a wavelength of 490 nm. Hereby the amount of the resulted colored formazan product is directly proportional to the amount of living and metabolic active cells.

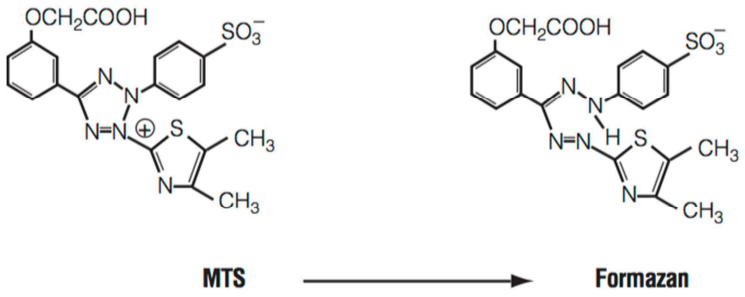

Figure 6. Structures of MTS tetrazolium and its reduced formazan product.
Source adapted from: (65).

Cell lines were plated into 96-well dishes. Using 3 x 10^3 cells per well for the T/C-28a2 chondrocyte cell line and 5 x 10^3 cells per well for the C28/I2 chondrocyte cell line seeded with their specific cell culture medium with FBS. The C28/I2 chondrocyte cell line was additionally treated with IL-1β [10 ng/ml] representing the osteoarthritic (OA) model.
The treatment was performed 24 hours after seeding with following concentrations of leptin [1.0 µg/ml, 0.5 µg/ml, 0.1 µg/ml, 0.01 µg/ml and 0.001 µg/ml]. A control was performed with 100 µM/ml diacerein. Test samples and diacerein control were performed in quadruplicates.
Measurements have been made 24 hours and 48 hours after the treatment, therefore 20 µl of CellTiter 96®Aqueous One Solution Reagent was added to each well and incubated for 3 hours (37°C, 5% CO_2). The color reaction was checked repeatedly. The absorbance values of the purple formazan products were measured at 490 nm with a Spektrostar NANO (BMG LabTech, Ortenberg, GER). Untreated cells were used as a control group.

2.5 Quantitative real- time Polymerase Chain Reaction

Since the 1980s when the Cetus Corporation researcher Kary Mullins developed the Polymerase Chain Reaction (PCR), his invention became one of the most used techniques in modern molecular biology (66). PCR is nowadays utilized for many interrogations like DNA cloning, detection of genome analysis, detection of viral and bacterial infections and various more.

PCR uses the ability of DNA polymerase to synthesize new DNA strands complementary to the strands utilized as template. Hereby nucleotides were only added to a preexisting

3´-OH group. Therefore a specific primer is required onto which the first nucleotide gets added by the DNA polymerase. Due to this specific binding condition it is possible to amplify a certain sequence of interest up to million times. The amplified sequences are referred to as amplicons.

The main components for PCR analysis are the DNA template as targeted sequence, a DNA polymerase for generating new complementary DNA strands, specific primers as starting points to amplify the targeted sequences and nucleotides (deoxynucleotide triphosphates - dNTPS). For real-time PCR analysis a specific fluorescent dye to measure the generated amplicons is additionally needed. Polymerase Chain Reactions can be explained, in a simplified approach, by these major processes (Figure 7).

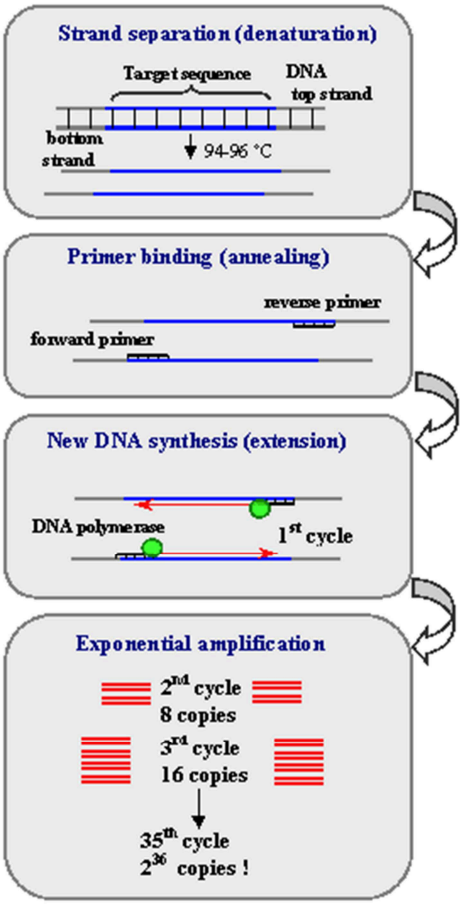

Figure 7. Polymerase Chain Reaction concept
First box: Denaturation (strand separation): dsDNA are melted to ssDNA by using high temperature incubation at 94 to 96°C. **Second box:** Annealing (primer binding): With an appropriate temperature for primer activity (approx. 60°C) complementary sequences were hybridized. **Third box:** Extension (new DNA synthesis): With the proper temperature of about 60°C the DNA polymerase works best to extend the primer indicated sequences. **Fourth box:** exponential amplification. Source adapted from: (67).

A more refined procedure is the real-time PCR, hereby the amount of amplicons is measured after every cycle via fluorescent dye that produces an increasing fluorescent signal in direct proportion to the amount of PCR product molecules. This enables to assess the PCR progress in real time. After each cycle the amplicons were measured whereas if the particular sequence occurs highly, it is detected in early cycles. In contrast sequences that are expressed rarely were identified in later cycles. In this study RT-qPCR was used to analysis the variances in extracellular matrix protein gene expressions of C28/I2 and T/C-28a2 chondrocyte cell lines after a specific leptin treatment (67–69).
The gene expression analyses via RT-qPCR were performed according to the 'Minimum Information for Publication of Quantitative Real-Time PCR Experiments'- Guidelines (MIQE- Guidelines) (70). These criteria imply to provide all relevant experimental conditions and assay characteristics and to give full disclosure of all reagents, sequences, and analysis methods. The aims of these guidelines are to enable publishers to create qPCR experiments with greater inherent value, to allow reviewers to measure the technical quality of the published studies and to provide an easier option to replicate the experiments in published studies (70). It is also an important step to maintain the necessary assessment of the technical adequacy of PCR-based publication (71).

The steps illustrated in chapter 2.5.1 up to chapter 2.5.4 were essentially performed prior to the Real-Time Polymerase Chain Reaction documented in 2.5.5.

2.5.1 RNeasy®- RNA Isolation

The RNeasy Mini Kit (Qiagen, Hilden, Germany) was used to purify total RNA. This assay kit is based on following steps. Cells were lysed to release all RNA contained. In a next step homogenizing was performed to create a homogenous lysate by grinding high-molecular-weight cellular components. Additionally in this step a highly denaturing guanidine-isothiocyanate-containing buffer was utilized, which ensures to isolate intact RNA by inactivating RNases. For ideal binding condition ethanol was added. Genomic DNA, cell debris, protein and other substances inhibiting the PCR process were removed by using spin columns (RNeasy Mini spin columns) with a special membrane (RNeasy silica membrane) in combination with a high-salt buffer. This membrane binds the RNA and in a next step all contaminations get washed off. At the end of the procedure pure RNA is available eluted into 30 µl of RNase-free water (Figure 8).

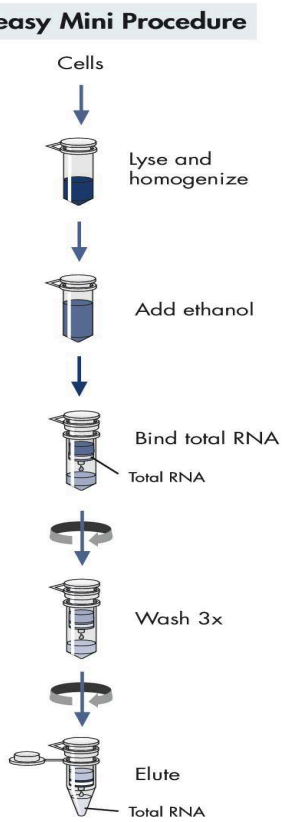

Figure 8. Schematic overview of RNA isolation
Source adapted from: (72).

2.5.1.1 Protocol

For this study $3x10^5$ cells were plated in 2 ml of their specific CCM into 6-well dishes 24 hours before treatment. The T/C-28a2, C28/I2 and C28/I2 + IL-1β [10 ng/ml] cell lines were treated with leptin [0.5 µg/ml; 0.2 µg/ml] versus a non-treated control group. All samples were made in duplicates. Total RNA was purified 24 hours and 48 hours after the treatment.

For setup preparation, 10 µl β-mercaptoethanol (β-ME) per 1.0 ml RLT Buffer (Qiagen, Hilden, Germany) was added and an ethanol was diluted to a solution [70%].

Cells were lysed and harvested after they were washed with 37°C PBS 1x (Gibco® life technologies™) by pipetting 175 µl RLT buffer + β-ME into each well of a duplicate. Duplicates were harvested and pooled by using a cell scraper and the pooled cells were transferred into spin columns prefilled with 350 µl ethanol [70%].

The spin columns were placed into a centrifuge (10.000 rpm; 30 seconds) past spinning the flow-through was discarded.

Next steps:

- 700 µl Buffer RW1 (Qiagen, Hilden, Germany) was added
    - Centrifuged at 10.000 rpm, 30 seconds, flow-through was discarded
- 500 µl Buffer RPE (Qiagen, Hilden, Germany) was added
    - Centrifuged at 10.000 rpm, 30 seconds, flow-through was discarded
- 500 µl Buffer RPE (Qiagen, Hilden, Germany) was added
    - Centrifuged at 10.000 rpm, 2 minutes, flow-through was discarded

For best results, the collection tubes were renewed and the membrane of the spin-columns were dried by spinning at 10.000 rpm for 1 minute. RNA was isolated and diluted with 30 µl of RNase-free water by a last spinning task at 10.000 rpm for 1 minute.

The total RNA concentration of each sample was quantified by using a NanoDrop 1000 spectrometer (Thermo Fisher Scientific, Waltham, U.S.A.). Prior to the measurement the spectrophotometer was calibrated with RNase-free water. Measurements were performed by pipetting 2 µl of each sample on the sample pedestal. Predicting a linear change in absorbance with concentration, the Beer-Lambert law is used to determine the concentration of RNA. RNA has its absorbance maximum at 260 nm. For concentration and purity analysis the absorbance at 280 nm is measured as well, due to the fact that, phenol, protein and other contaminations absorb strongly or near 280 nm. Using the ratio of the 260 nm and 280 nm absorbance the RNA purity was assessed. A 260/280 ratio of 1.8 to 2.0 is identified for pure RNA. All RNA samples were stored at -70°C (73).

2.5.2 Bio Analyzer – quality assessment of total RNA

The quality assessment of the purified total RNA was performed with an Agilent 2100 BioAnalyzer (Agilent Technologies, Santa Clara, U.S.A.).

The Agilent 2100 BioAnalyzer is a complex system with a “lab on chip” procedure based on capillary electrophoresis and fluorescent dye binding on RNA strands. With this system the total RNA concentration and RNA integrity was measured.

The chip contains sample wells, gel wells and a reference standard well filled with fluorescence dye and a sieving polymer matrix. Once the wells are prepared the chip gets integrated in an electric circle. Charged RNA is electrophorically driven by a voltage

gradient and is separated by size due to the mass-to-voltage ratio and the polymer matrix. Furthermore the dye molecules linked to the RNA strands were measured by a laser induced fluorescence. The data of the unknown samples were translated into gel-like images (bands) and electropherograms (peaks) and compared to the ladder for identifying rRNA peaks. For a better reproducibility an unitless number (1-10) based on a software algorithm using all electrophoretic traces was invented. The RNA Integrity Number (RIN) indicates 1 for the most degraded RNA and 10 for the most intact RNA. All RNA samples in this study were detected with a RIN between 9.8 and 10.

The concentration and purity of each RNA sample was determined by using 1µl of each sample for testing runs according to the manufacture´s protocol for the Agilent 2100 BioAnalyzer (Agilent Technologies) (73).

2.5.3 Removal of genomic DNA

For the essential preparation of DNA-free RNA prior to the RT-PCR, the Thermo Scientific™ DNase I, RNase-free kit (Thermo Fisher Scientific) was utilized.
The DNase I, RNase-free is a 29 kDa monomer belonging to the group of endonucleases. The enzyme digests single- and double-stranded DNA (ssDNA; dsDNA) by hydrolyzing phosphodiester bounds producing mono- and oligodeoxyribonucleotides with 5´-phosphate and 3´-OH groups. The enzyme activity factually depends on the presence of Ca^{2+} and gets activated by Mg^{2+} ions.

The provided 10x reaction buffer with $MgCl_2$ contains 100 mM Tris-HCl (pH 7.5 at 25°C), 25 mM $MgCl_2$ and 1 mM $CaCl_2$. According to the BioAnalyzer Data (2.5.2.) 1 µg purified RNA (in a maximum volume of 8 µl) was added to 1 µl 10x reaction buffer with $MgCl_2$ and 1 µl DNAse I, RNase-free. Diethylpyrocarbonate-treated water (DEPC-treated and therefore RNase-free) was used to obtain the claimed total volume of 10 µl, if necessary.
Past these steps the composite (in total 10 µl) was incubated at 37°C for 30 minutes to start the digesting process of the ssDNA and dsDNA.
Next 1 µl ethylenediaminetetraacetic acid (EDTA) [50 mM] was added to stop and inactivate the enzyme. The samples were incubated at 65°C for 10 minutes in presence of EDTA [50 mM].

2.5.4 Complementary DNA Synthesis

For the synthesis of complementary DNA (cDNA) the iSCript™ cDNA Synthesis Kit (BioRad Laboratories, Hercules, U.S.A.) was used.

The provided iScript™ reverse transcriptase (BioRad) is a modified Moloney Murine Leukema Virus-derived (MMLV-derived) reverse transcriptase, which has an optimal sensitivity for quantitative PCR. Additionally the enzyme was preblended with an RNase inhibitor for best performance of transcription. The other provided reagent a 5x iScript™ reaction mix (BioRad) is a blend of oligo deoxy-thymidine nucleotides (dT) and random hexamer primers.

The RNA template (11 µl) was added to 1 µl iScript™ reverse transcriptase, 4 µl 5x iScript™ reaction mix and 4 µl nuclease-free water to a total volume of 20 µl. The composite was processed according to the reaction protocol, shown in Table 2.

Time (minutes)	Temperature (°C)
5	25
30	42
5	85
Hold	4

Table 2. Reaction protocol for cDNA synthesis.

2.5.5 Real Time – quantitative Polymerase Chain Reaction

The real-time PCR reactions were performed in triplicates using the SsoAdavanced™ Universal SYBR® Green Supermix (BioRad) with a CFX96 Touch Real-Time PCR Detection System (BioRad). This SYBR® mixture contains antibody-mediated hot-start Sso7d-fusion polymerase, dNTPs, $MgCl_2$, SYBR® Green I dye, enhancers, stabilizers and a blend of passive reference dyes.

The principle of DNA detection with SYBR® Green I dye is shown in Figure 9 and 10.

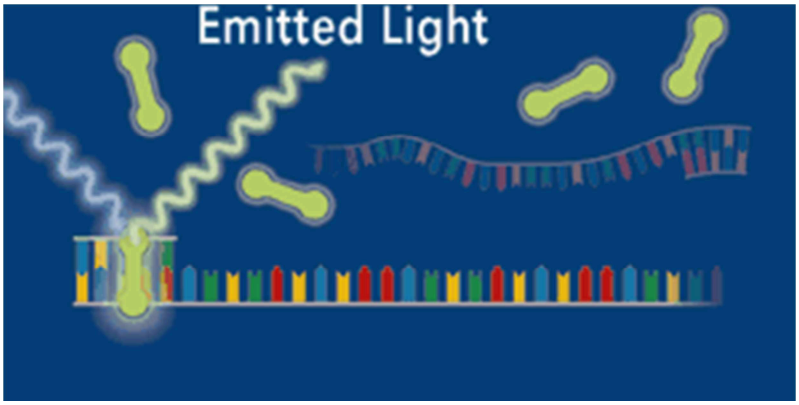

Figure 9. SYBR Green I Dye during the annealing phase
SYBR Green I Dye binds to double-strained DNA. Source adapted from: (74).

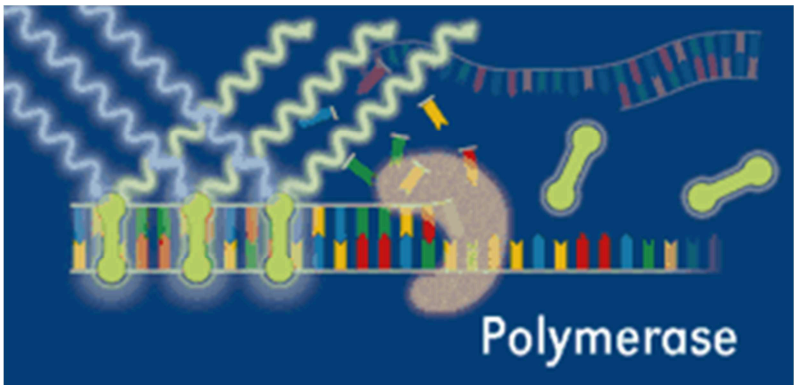

Figure 10. SYBR Green I Dye during the extension phase
In the extension phase more and more SYBR Green I Dye binds to the amplicons, resulting in an increased fluorescence. The amount of newly generated amplicons is in a direct proportion of the increased fluorescence. At the end of amplification, when the double-strained DNA gets denatured to single-strained DNA, the fluorescence dye is liberated, and the fluorescence signal decreases. Source adapted from: (74).

The following primers were applied for RT-PCR:

- QuantiTect® primer assays (Qiagen, Hilden, Germany) as reference genes:
  - β-Actin (ACTB, QT00095431)
  - Hypox anthine phosphoribosyl-transferase (HPRT-1, QT00059066)
  - Glyceraldehyde 3-phosphate dehydrogenase (GAPDH, QT00079247)

- QuantiTect® primer assays (Qiagen, Hilden, Germany) for Col1A1 and LAMA analysis:
  - COL1A1 (QT00037793)
  - LAMA4 (QT00032977)

- Eurofins MWG Operon (Ebersberg, Germany) forward and reverse primers for Col2A1 analysis (Table 3):

Oligo Name	Sequence (5´→ 3´)	ID
hCollagen2fwd	CTATCTGGACGAAGCAGCTGGCA (23)	ID012584801
hCollagen2rev	ATGGGTGCAATGTCAATGATGG (22)	ID012584802

Table 3. Primers used for collagen 2A1 analysis

- Eurofins MWG Operon (Ebersberg, Germany) forward and reverse primers for matrix metalloproteinase (MMP) analysis (Table 4):

Oligo Name	Sequence (5´→ 3´)	ID
MMP-1 fw	CTGTTCAGGGACAGAATGTGCT (22)	ID012454277
MMP-1 rev	TCGATATGCTTCACAGTTCTAGGG (24)	ID012454278
MMP-3 fw	TTTTGGCCATCTCTTCCTTCA (21)	ID012454281
MMP-3 rev	TGTGGATGCCTCTTGGGTATC (21)	ID012454282
MMP-9 fw	GGGACGCAGACATGTCATC (20)	ID012454283
MMP-9 rev	TCGTCATCGTCGAAATGGGC (20)	ID012454284
MMP-13 fw	TCCTCTTCTTGAGCTGGACTCATT (24)	ID012454287
MMP-13 rev	CGCTCTGCAAACTGGAGGTC (20)	ID012454288

Table 4. Primers used for MMP analysis

The reaction setup for the QuantiTect® primer assays is shown in Table 5.

Reagent	Volume (µl)
Sso Advanced universal SYBR® Green supermix (2x)	5
Quantitect Primer (10x)	1
NFW (nuclease free water)	3
Template (3,125ng)	1
	Total 10

Table 5. Reaction setup for QuantiTect Primers.

The reaction setup for Eurofins MWG Operon was performed according to Table 6.

Reagent	Volume (µl)
Sso Advanced universal SYBR® Green supermix 2x	5
Forward (fw) Primer [200 nm/µl]	1
Reverse (rv) Primer [200 nm/µl]	1
NFW (nuclease free water)	2
Template (3,125ng)	1
	Total 10

Table 6. Reaction setup for the combined forward and reverse primer mixture.

All components were pipetted with utmost diligence into the wells of a PCR plate according to Table 5 and Table 6. In a next step the wells were sealed with an optically transparent film, and vortexed thorough to ensure all components were mixed well. PCR plates were centrifuged at 900 rpm for 1 minute prior they were loaded into the CFX96 Touch Real-Time PCR Detection System (BioRad). According to the MIQE guidelines (70) melt curve and peak analyses (Figure 12) were performed in order to determine the specificity of the amplification. The thermal cycling protocol was programed as illustrated in Figure 11. The data analysis was finally performed by the instrument- specific instructions as recommended.

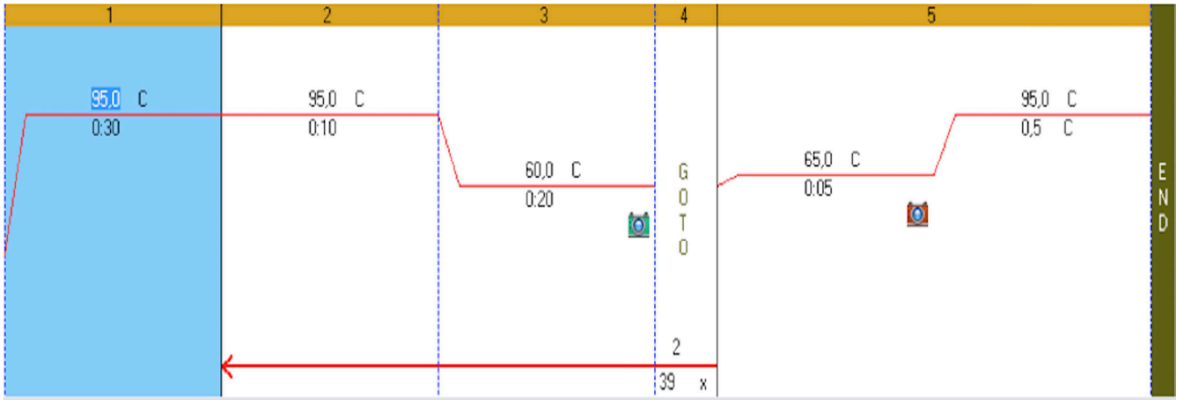

Figure 11. Thermo cycling protocol
Performed with BioRad CFX96 Touch system for collagen and MMP gene analysis (setting: SYBR Green) 1. Polymerase activation and DNA denaturation (95°C, 30 sec) 2. Denaturation (95°C, 10 sec) 3. Annealing/ Extension and plate read (60°C, 20 sec) 4. Cycling repeat starting from point 2. up to 39 times. 5. Melt curve analysis (65°C to 95°C) and plate read.

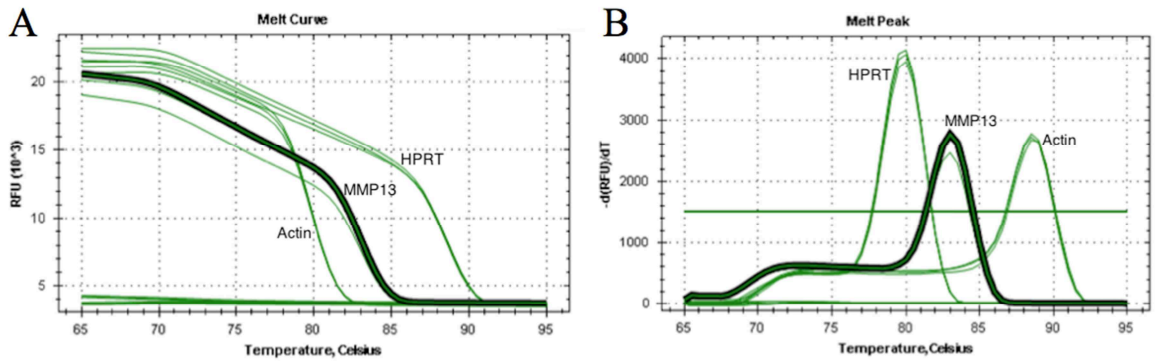

Figure 12. Melting curve and peak analysis to determine specifity of the amplification
A: Melt curves of reference genes (Actin, HPRT) and MMP-13, showing the correlation of temperature and fluorescence of each gene. Fluorescence is only given when the intercalating dye is bound to dsDNA, increasing temperature leads to denaturation of dsDNA to single-stranded DNA, followed by a fluorescence decrease. **B:** For a better assessment the first negative derivative is used to point out the dissociation temperatures for HPRT (at 60°C), MMP-13 (63°C) and Actin (89°C). Additionally the single peaks can be interpreted as pure, single amplicons.

Following the RT-PCR analysis the expression level (C_T) of the target gene was normalized to the reference genes (GAPDH, ACTB, and HPRT-1) (ΔC_t) and then the ΔC_t of the test sample was normalized to the ΔC_t of the controls ($\Delta\Delta C_t$). Finally, the expression ratio was calculated with the $2^{-\Delta\Delta Ct}$ method ($^*P < 0.05$) (75).

2.6 SIRCOL™- soluble collagen assay

Sircol™- soluble collagen assay (Biocolor, Carrickfergus, UK) is a colorimetric method to analysis the amount of acid-soluble collagens in experimental setups. The assay was performed to gain information about the newly synthesized collagen from C28/I2 ± IL-1β and T/C-28a2 chondrocyte cell lines in a pro-inflammatory environment. The inflammatory condition was set by leptin in a concentration of 0.5 µg/ml. Measurements were performed 24 hours and 48 hours past the treatment and incubation with leptin. The assay is based on a dye-binding method; the Sircol Dye Reagent (Figure 13) binds soluble collagens and can be related and analyzed with the reference standards after a colorimetric measurement.

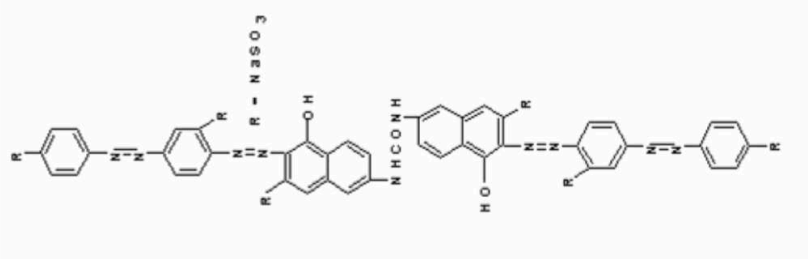

Figure 13. Molecular structure of Sircol Dye (Sirius Red)
Source adapted from: (76)

As reference standards (Biocolor) a sterile solution of cold-acid soluble collagen Type [500 µg/ml bovine and rat collagen] in a 0.5 M acetic acid was used. For best results the absorbance values of the test samples, reference standards and blanks must be measured at a wavelength of 555 nm with a 96-well plate reader (Figure 14)

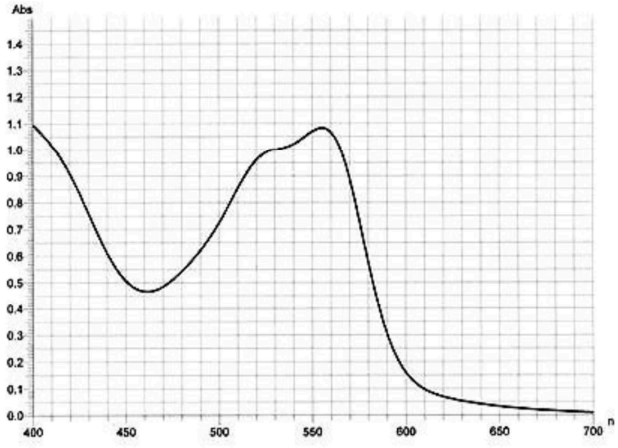

Figure 14. Sircol absorbance spectrum
The absorbance maximum is detected at a wavelength of 555 nm. Source adapted from: (76)

2.6.1 Protocol

The T/C-28a2 and C28/I2 ± IL-1β [10ng/ml] chondrocyte cell lines were seeded in 6-well plates 24 hours before the treatment. For ideal conditions regarding confluence and growth space 2.5 x 10^5 cells per well were used. Before the treatment with leptin, cell culture medium was removed and cells were washed with 37°C PBS 1x (Gibco). The treatment was performed with a leptin concentration of 0.5 µg/ml versus a non-treated control group. The Sircol assay was performed 24 hours and 48 hours past the treatment and incubation with leptin.

Set up preparation:

- A set of 1,5 ml Protein LoBind tubes (Eppendorf, Hamburg, Germany) was labeled
- Blanks (100 µl) were prepared in duplicates from a mixture of 1000 µl distilled water, 100 µl acid neutralizing reagent (Biocolor), 200 µl isolation and concentration reagent (Biocolor)
- Reference standards (Biocolor) were compounded in duplicates according to Table 7 and Figure 15.

Standards	Reference standard (µl)	Fill up to 100 µl with blank (µl)
S1- [15 µg]	10	90
S2- [10 µg]	20	80
S3- [15 µg]	30	70
S4- [20 µg]	40	60
S5- [25µg]	50	50
S6- [30µg]	60	40

Table 7. Sircol reference standards

Assay procedure:

- The cell culture medium was removed carefully and cells were rinsed with 37°C warm PBS 1x. An additive isolation and concentration step was performed to free the acid-soluble collagens, therefore 1 ml 4°C cold Acetic Acid [0.5 M] was added to every sample. Additionally the samples were placed on a mechanically shaking plate at room temperature [approx. 21- 23°C] (rt) for 5 minutes.
- After the incubation 1.0 ml supernatant was carefully transferred to the Protein LoBind tubes (Eppendorf) by using a pipette. Next 100 µl acid neutralizing reagent (Biocolor), which contains Tris-HCl and NaOH was added. As well as 200 µl isolation and concentration reagent (Biocolor), which contains polyethylene glycol in a Tris-HCl buffer, pH 7.6. Hereafter an overnight storage and incubation at 4°C had to be performed.
- Past the overnight incubation the samples were placed strictly without shaking and without delay in a centrifuge (12.000 rpm; 10 minutes). Afterwards 1000 µl supernatant was attentively removed not affecting the pellet by using a pipette and the assay was continued with the remaining supernatant and the pellet.

- 1 ml Sircol Dye Reagent (Biocolor) was added to each microcentrifuge tube and mixed by inverting. The samples were additionally placed on a mechanically shaking plate (rt) for 30 minutes. Accordingly the samples were centrifuged at 12.000 rpm for 10 minutes and the tubes were carefully inverted and drained, avoiding any pellet loss.
- The pellets of each sample were mixed with 750 µl ice-cold acid-salt wash reagent (Biocolor) containing acetic acid, sodium chloride and surfactans. Following 10 minutes at 12.000 rpm in a centrifuge, the wash was discarded and any fluids were removed for optimal results.
- In a final step 250 µl alkali reagent (Biocolor) containing 0.5 M sodium hydroxide was added and the bound dye was dissolved properly by using a vortex shaker.
- The dissolved bound dye of each sample was now pipetted (200 µl per well) in a 96-well dish and measured at 555 nm with a Spektrostar NANO (BMG LabTech, Ortenberg, GER) (Figure 15)

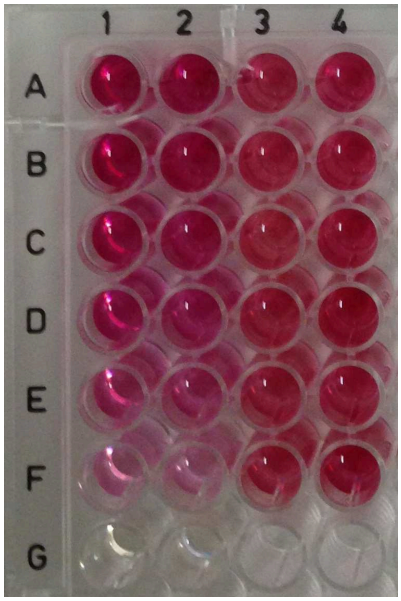

Figure 15. Sircol pipetting layout
Wells: A1-2 Standard [30µg], B1-2 Standard [25µg], C1-2 Standard [20µg], D1-2 Standard [15µg], E1-2 Standard [10µg], F1-2 Standard [5µg], G1-2 Blanks. Wells: A3-4 to F3-4 specific samples according to protocol. Source: FH

2.7 BLYSCAN™- sGAG analysis

The Blyscan™ - sulfated Glycosaminoglycan assay (Biocolor, Carrickfergus, UK) is used for quantitative analyses of sulfated glycosaminoglycan (sGAG), a major component of the extracellular matrix. The colorimetric technique uses a quantitative dye-binding method; hereby 1,9-dimethyl-methylene blue (Figure 16) is set to be the specific label, when the blue dye turns into a bright pink indicating sulfated glycosaminoglycan chains.

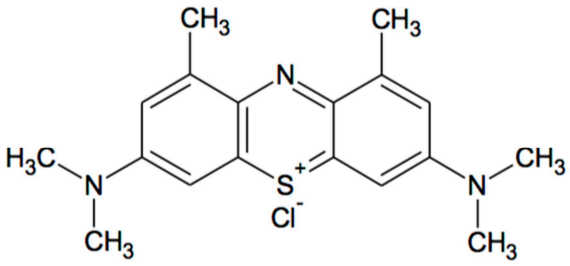

Figure 16. Molecular Structure of Blyscan Dye
Source adapted from: (77)

In this trial Blyscan™- sGAG assay was utilized to obtain information about sulfated Glycosaminoglycan after a papain extraction from leptin treated T/C-28a2 and C28/I2 ± IL-1β [10 ng/ml] chondrocyte cells lines.

The treatment was performed with a leptin concentration of 0.5 µg/ml versus a non-treated control group. Measurements were realized 24 hours and 48 hours after the treatment and incubation with leptin.

As reference standards (Biocolor) a sterile solution of bovine tracheal chondroitin 4-sulfate [100 µg/ml] was applied. For best results the absorbance values of the test samples, reference standards and blanks were measured at a wavelength of 656 nm with a 96-well plate reader (Figure 17).

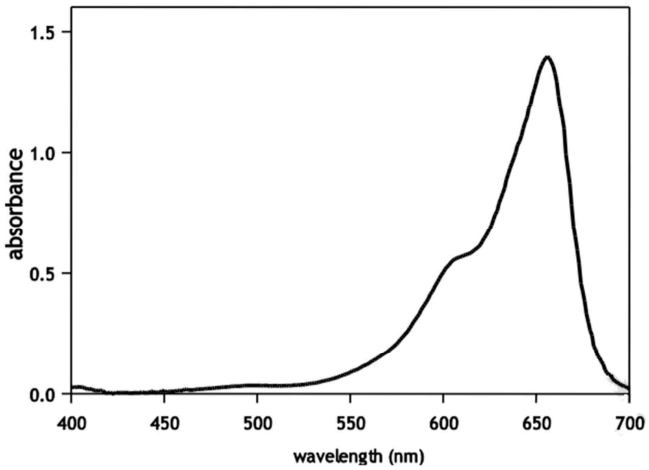

Figure 17. Blyscan Absorbance Spectrum
The absorbance optimum is determined at a wavelength of 656 nm.
Source adapted from: (77)

2.7.1 Protocol

Chondrocyte cell lines were plated into 6-well dishes 24 hours before the treatment (2.5 x 10^5 cells per well). T/C-28a2 and C28/I2 ± IL-1β [10 ng/ml] chondrocyte cell lines were treated with leptin [0.5 µg/ml] versus a CCM control group. Photometric measurements were performed at 24 hours and 48 hours past the leptin treatment.

Set up preparation:

- The Papain Extraction Reagent needed for this analysis was prepared according to the manufacture´s protocol listed below:
    - To 50 ml of a 0.2 M sodium phosphate buffer (pH 6.4), 400 mg sodium acetate, 200 mg EDTA disodium salt, 40 mg cysteine HCl and 250 µl papain suspension [5mg enzyme per 250 µl] (Sigma Aldrich, St. Louis, U.S.A.) were added.
- A set of set of 1,5 ml Protein LoBind tubes (Eppendorf) were labeled and blanks were prepared in duplicates of 100 µl cell culture medium as well as the reference standards (Biocolor) were prepared in duplicates (Figure 18) and (Table 8).

Standards	Reference standard (µl)	Fill up to 100 µl with CCM (µl)
S1- [1 µg]	10 µl	90
S2- [2 µg]	20 µl	80
S3- [3 µg]	30 µl	70
S4- [4 µg]	40 µl	60
S5- [5 µg]	50 µl	50

Table 8. Reference standards Blyscan

Assay procedure:

- Cell culture medium was removed carefully and the samples were rinsed with 37°C warm PBS 1x. In a next step 600 µl buffer (Papain Extraction Reagent) was pipetted into every well and incubated for 3 hours at 65°C.
- After 3 hours of incubation the samples were placed on mechanically shaking plate (rt) for 1 minute and the supernatants of each well were transferred carefully to the microcentrifuge tubes and were centrifuged at 10.000 rpm for 10 minutes.
- Past these steps the assay was continued with 33 µl of the generated extract plus 66 µl distilled water as test samples (100 µl). To each tube 1.0 ml Blyscan Dye Reagent (Biocolor) containing 1,9-dimethyl-methylene blue in organic buffer including surfactants was added. Samples were mixed by inverting and additionally placed on a mechanically shaking plate (rt) for 30 minutes. Subsequently the samples were centrifuged at 12.000 rpm for 10 minutes and the tube were carefully inverted and drained, any fluids still remaining were removed by gently tapping the inverted tube on paper towel, avoiding any pellet loss.
- 500 µl Dissociation Reagent (Biocolor) containing sodium salt of an anionic surfactant was added and the bound dye was dissolved properly by using a vortex shaker after that the samples were centrifuged one final time at 12.000 rpm for 5 minutes
- For the measurement 200 µl of each sample were pipetted into a well of a 96-well plate and measured at 656 nm with a Spektrostar NANO (BMG LabTech) (Figure 18).

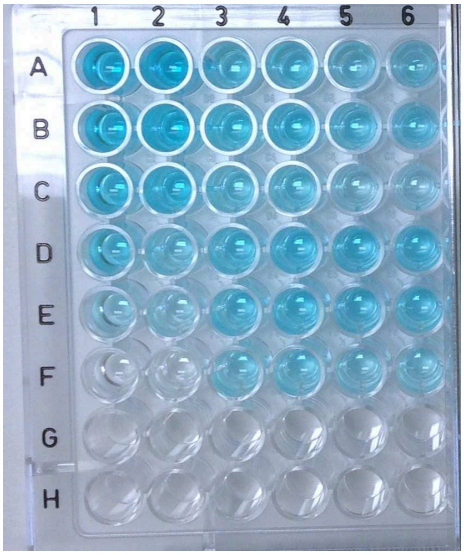

Figure 18. Blyscan assay (96-well plate)
A1-2 to E1-2: aliquots containing 5 µg (A1-2) to 1µ (E1-E2) of reference standard; F1-2: blanks; A3 – F6: specific test samples according to protocol. Source: FH

2.8 Statistical analysis

All values are expressed as mean values ± standard deviation (SD). A student´s unpaired t-test was performed to assess differences between the leptin treated groups and their particular control groups. The significance of dose or time response was assessed by repeated measure analysis. The graphic data were established and calculated with Sigma Plot® (Systat Software Inc., San Jose, U.S.A.).

3 Results

3.1 Short Tandem Repeat- analysis

The STR analysis was performed with a PowerPlex 16® System in order to confirm, that the C28/I2 and T/C-28a2 cell lines are obtained from the same patient and therefore to achieve comparability and reproducibility of the experiments based on an OA model versus a non-OA model (Table 9).

STR locus	C28/I2 (p7)	T/C-28a2 (p7)
D3S1358	15,2	15,2
TH01	9,3	9,3
D21S11	26.2/28.2	28.2, 30.2
D18S51	16	16,19
Penta E	7	7,11
D5S818	11	11,12
D13S317	9,11	11
D7S820	8,10	8,10
D16S539	12,13	12,13
CSF1PO	12	12,13
Penta D	14	14
Amelogenin	x	x
vWA	14	14,18
D8S1179	11,13	11,13
TPOX	8	8
FGA	20	20

Table 9. STR loci comparison of C28/I2 and T/C-28a2

C28/I2 and T/C-28a2 cell lines match in the following 16 STR loci as shown in Table 9.: D3S1358; TH01; D21S11; D18S51; Penta E; D5S818; D13S317; D7S820; D16S539; CSF1PO; Penta D; Amelogenin; vWA; D8S1179; TPOX; FGA. The results affirm the same origin of the C28/I2 and T/C-28a2 cell lines.

3.2 Vimentin-DAPI Immunofluorescence analysis

The vimentin-DAPI immunofluorescence screening was performed in order to confirm the mesenchymal origin of the C28/I2 and T/C-28a2 cell lines (Figure 19) and (Figure 20). Based on a high vimentin expression marked by the green immunofluorescence respond in Figure 19 B, C and Figure 20 B, C, the mesenchymal origin of the chondrocyte cell lines was verified.

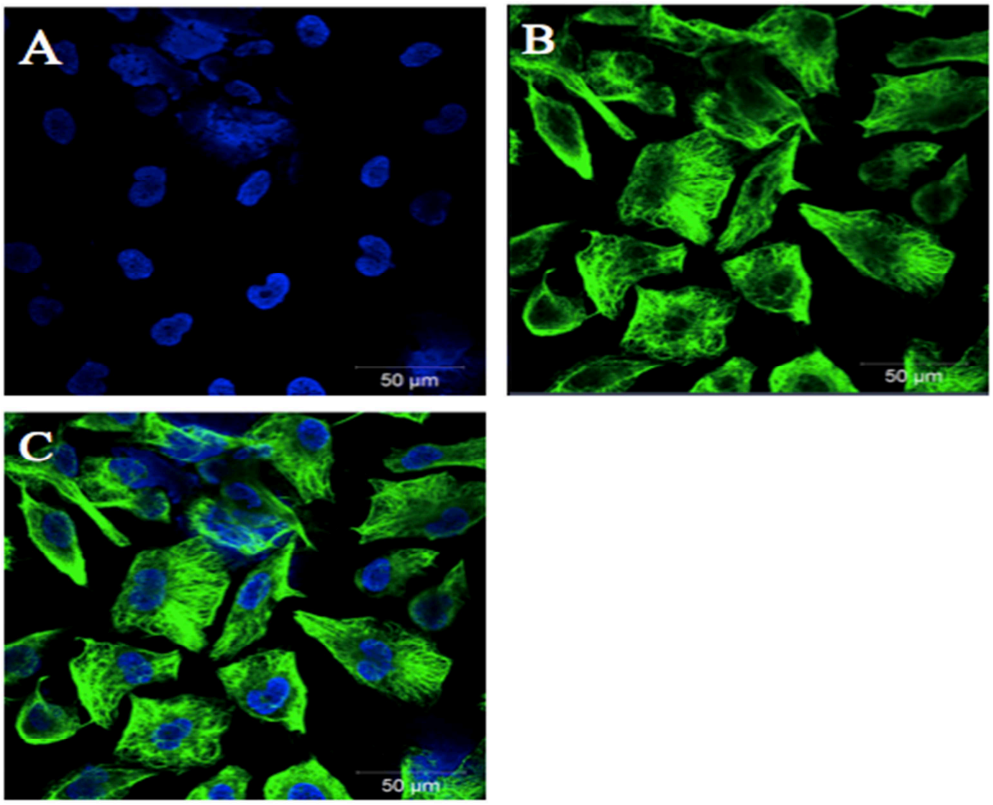

Figure 19. Vimentin-DAPI immunofluorescence of the C28/I2 cell line
A: Nuclei were stained with DAPI; **B:** High vimentin expression confirming the mesenchymal origin of C28/I2; **C:** Nuclei (blue) and vimentin expression (green) in an overlay imaging.

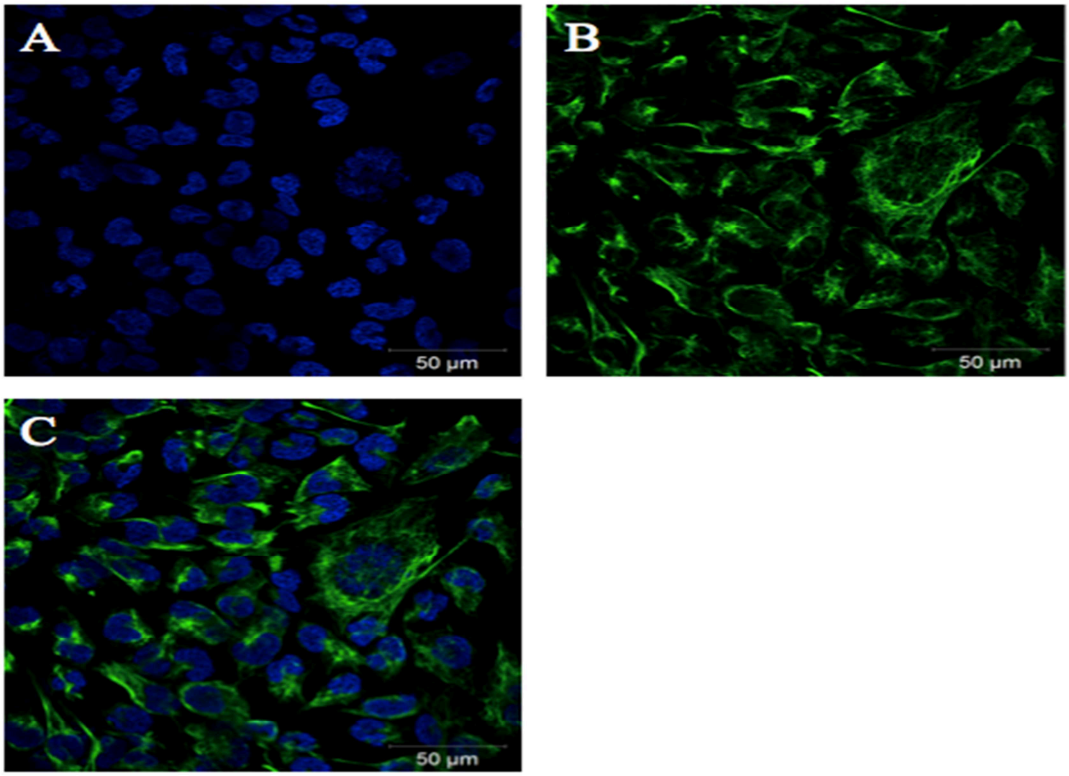

Figure 20. Vimentin-DAPI immunofluorescence of the T/C-28a2 cell line
A: Nuclei were stained with DAPI; **B:** High vimentin expression confirming the mesenchymal origin of T/C-28a2; **C:** Nuclei (blue) and vimentin expression (green) in an overlay imaging.

3.3 xCELLigence- cell viability assessment

An xCELLigence System was used, in order to determine the growth behavior in presence and absence of foetal bovine serum (FBS) and varied quantities of seeded cells (Figure 21). 3000 and 5000 cells/well were plated into a 16-well E-plates® (Roche Diagnostics) in specific CCM including FBS or no FBS. The growth behavior was recorded for 77h. The RTCA 1.2.1. Software was utilized to calculate the population doubling time of the C28/I2 + IL-1β and T/C-28a2 cell lines at 37°C in a humidified atmosphere (Table 11).

C28/I2 + IL-1β and T/C-28a2 chondrocyte cell lines need FBS to grow regularly. The analysis confirmed, that C28/I2 + IL-1β (3000 cells/well) plated with FBS as well as plated with 5000 cells/well containing FBS, have a better growth behavior and a faster doubling time, compared to the wells with the same amount of seeded cells without FBS (Figure 21 A). All doubling times were listed in Table 10.

Same results revealed the analysis of the T/C-28a2 cell line (Figure 21 B). Whereby the best growth behavior and fastest doubling time (13.8 h) was detected for wells seeded with 3000 cells containing FBS, followed by wells plated with 5000 cells including FBS. T/C-28a2 cells plated without FBS regardless the quantity of seeded cells, showed very little, up to no growth behavior (Figure 21 B) and (Table 10).

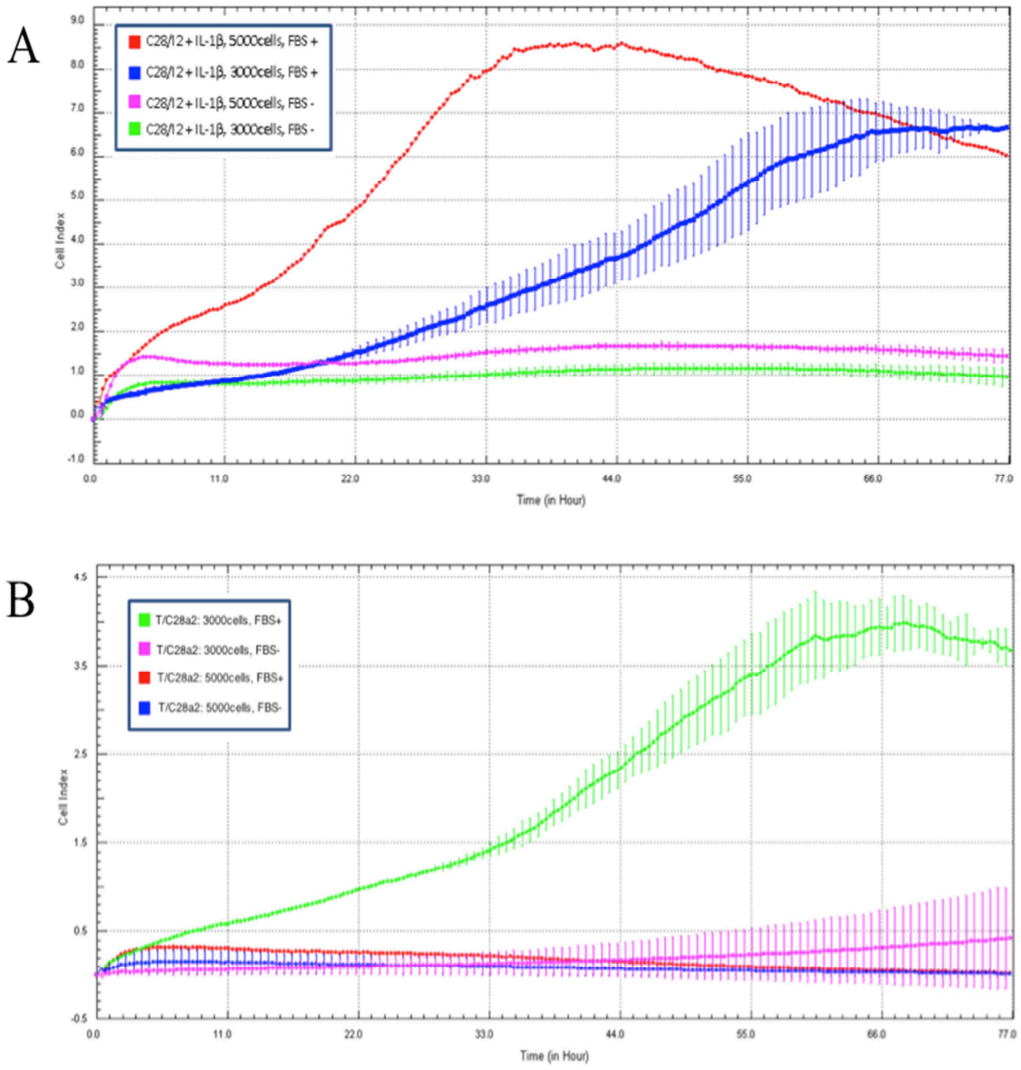

Figure 21. Real time growth measurement of C28/I2 + IL-1β and T/C-28a2
A: xCelligence Real Time growth measurement of C28/I2 + IL-1β, **red:** 5000 cells/well + FBS, **blue:** 3000 cells/well +FBS, **purple:** 5000 cells/well – FBS, **green:** 3000 cells/well – FBS; **B**: xCelligence Real Time growth measurement of T/C-28a2, **red:** 5000cells/well + FBS, **blue:** 5000 cells/well - FBS, **purple:** 3000 cells/well – FBS, **green:** 3000 cells/well + FBS

Population doubling times (DT)			
Cell line	**Cells/well**	**FBS - / +**	**DT [h]**
C28/I2 + IL-1β	3000	-	42.4
C28/I2 + IL-1β	3000	+	14.9
C28/I2 + IL-1β	5000	-	48.5
C28/I2 + IL-1β	5000	+	22.3
T/C-28a2	3000	-	n/a
T/C-28a2	3000	+	13.8
T/C-28a2	5000	-	n/a
T/C-28a2	5000	+	18.8

Table 10. Population doubling times of the C28/I2 + IL-1β and T/C-28a2

3.4 MTS cell viability assay

Chondrocytes were treated with recombinant leptin [0.001 µg/ml; 0.01 µg/ml; 0.1 µg/ml; 0.5 µg/ml; 1.0 µg/ml] for 24 h and 48 h; untreated cells were used as control group. After the respective time periods cells were incubated with a MTS tetrazolium compound and the newly produzed purple formazan product was measured spectrophotometrically [490 nm] to define cell viability.

The MTS tests (n= 2) indicated, that the leptin treatment has no significant negative effect on the cell viability of the C28/I2 and T/C-28a2 chondrocyte cell lines (Figure 22). Results are mean ± standard deviation of two independent experiments measured in quadruplicates.

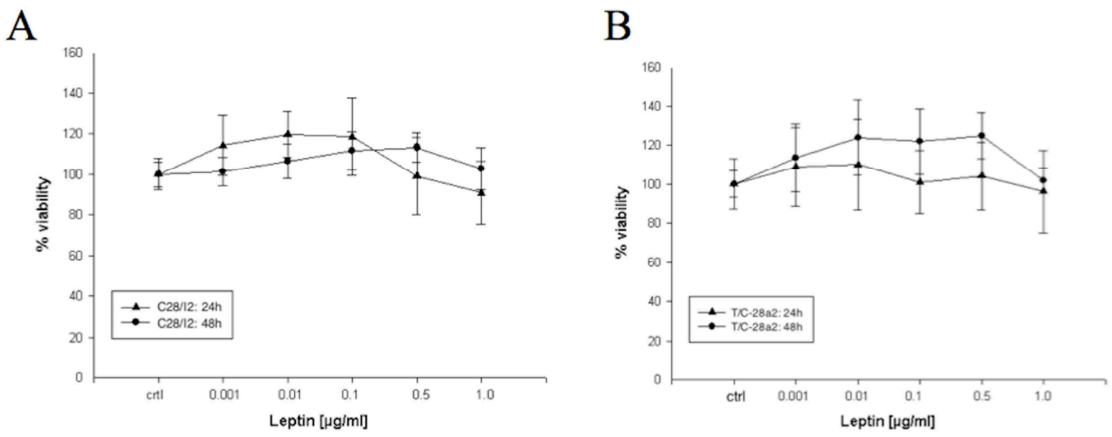

Figure 22. Cell viability assessment (24h and 48 h) of C28/I2 and T/C-28a2
A: Cell viability assessment of the C28/I2 cell line performed at 24 h and 48 h. **B:** Cell viability assessment of the T/C-28a2 performed at 24 h and 48 h.

3.5 Real- Time PCR analysis

In order to gain information about the gene expression levels of matrix metalloproteinases (MMPs) and collagens expressed by C28/I2 + IL-1β and T/C-28a2 real-time PCR analyses (n= 10) were performed.

The quality of the purified RNA was assessed with an Agilent BioAnalyzer 2100 (Agilent Technologies) which indicated a RIN between 9.8 and 10 (Figure 23) and (Figure 24). real-time PCR was performed according to the MIQE guidelines (70) 48 h after the treatment with leptin [0.2 µg/ml; 0.5 µg/ml]. Results are mean ± SD of 10 independent experiments carried out in triplicates.

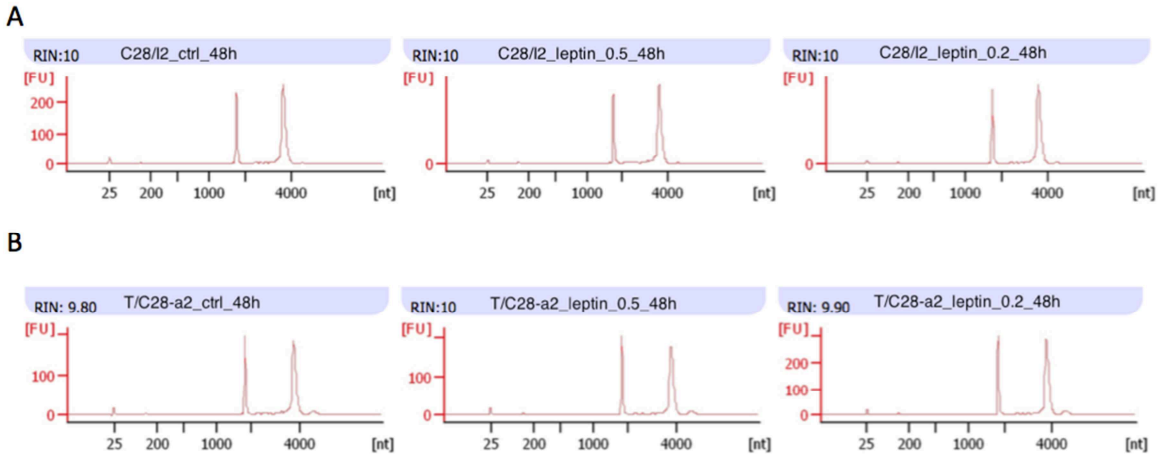

Figure 23. Representative Data of one experiment (BioAnalyzer 2100)
A: RNA analysis of C28/I2, left: control, middle: treated with leptin [0.5 µg/ml], right: treated with leptin [0.2 µg/ml], first peak: 18S ribosomal peak, second peak 28S ribosomal peak, small peaks in front: 25nt internal marker, 5S subunits, tRNA. **B:** RNA analysis of T/C-28a2, left: control, middle: treated with leptin [0.5 µg/ml], right: treated with leptin [0.2µg/ml], first peak: 18S ribosomal peak, second peak: 28S ribosomal peak, small peaks in front: 25nt internal marker, RNA, 5S subunits, tRNA. (FU= fluorescence units, nt= nucleotides)

The BioAnalyzer 2100 software uses the information shown in Figure 23 and illustrated in the corresponding electrophoresis analysis (Figure 24) to calculate the RIN via internal algorithm. The calculated RIN for C28/I2 + IL-1β treated with leptin [0.2 µg/ml; 0.5 µg/ml] as well as in the control group is detected to be 10 (Figure 23 A). The RIN analyzed for the T/C-28a2 control group was displayed at 9.80. T/C-28a2 treated with leptin [0.2 µg/ml] has a calculated RIN of 10. The RIN for T/C-28a2 [0.5 µg/ml] is detected at 9.90 (Figure 23 B).

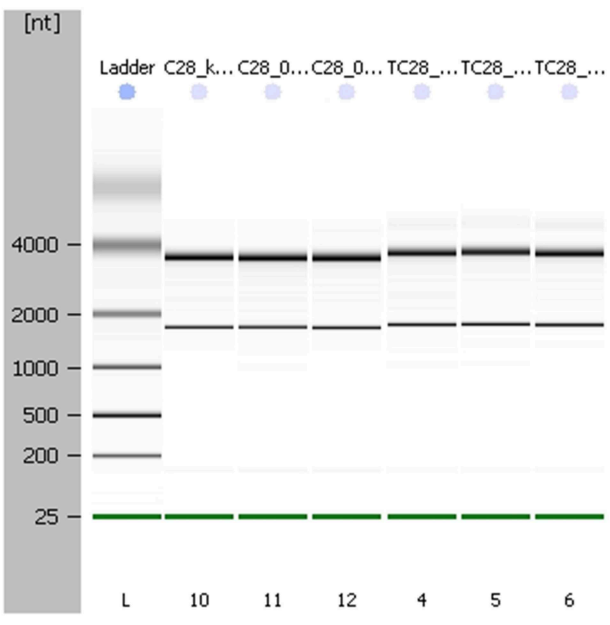

Figure 24. Corresponding BioAnalyzer 2100 Electrophoresis runs (gel files)
L= ladder, 10= C28/I2 (control), 11= C28/I2 (leptin 0.5 µg/ml), 12= C28/I2 (leptin 0.2 µg/ml) and 4= T/C-28a2 (ctrl), 5= T/C-28a2 (leptin 0.5 µg/ml), 6= T/C-28a2 (leptin 0.2 µg/ml) analyzed and compared to the ladder (left lane), top bands: 28S RNA strands, bottom bands: 18S RNA strands. Green: 25nt internal marker for correct analysis (nt= nucleotides)

3.5.1 Matrix Metalloproteinases (MMP) analysis

MMP-1: The gene expression level of MMP-1 expressed by C28/I2 + IL-1β showed increasing tendency which depends on an increasing leptin concentration. The T/C-28a2 cell line indicated a significant decrease (p= 0.035) at a leptin concentration of 0.2 µg/ml and a non-significant increase at a leptin concentration of 0.5 µg/ml (Figure 25 A, Table 11 and 12).

MMP-3: The C28/I2 + IL-1β cell line showed a non-significant increase of MMP-3 gene expression at the leptin [0.2 µg/ml] concentration, and a decrease with a leptin concentration of 0.5 µg/ml. MMP-3 genes expressed by the T/C-28a2 cell line indicated an non-significant decrease after the treatment with leptin [0.2 µg/ml] and no effect past the leptin [0.5 µg/ml] treatment (Figure 25 B, Table 11 and 12).

MMP-13: The analysis of the C28/I2 + IL-1β cells showed an increasing tendency of MMP-13 gene expression in connection with an increasing leptin concentration. MMP-13 genes expressed by the T/C-28a2 cell line indicated a significant decrease (p= 0.038) after

the treatment with leptin [0.2 µg/ml] and a non-significant decrease past the treatment with leptin [0.5 µg/ml] (Figure 25 C, Table 11 and 12).

The gene expression of MMP-9 was analyzed as well, but the expression levels were to low (cycle > 32) to analyze them with PCR methods.

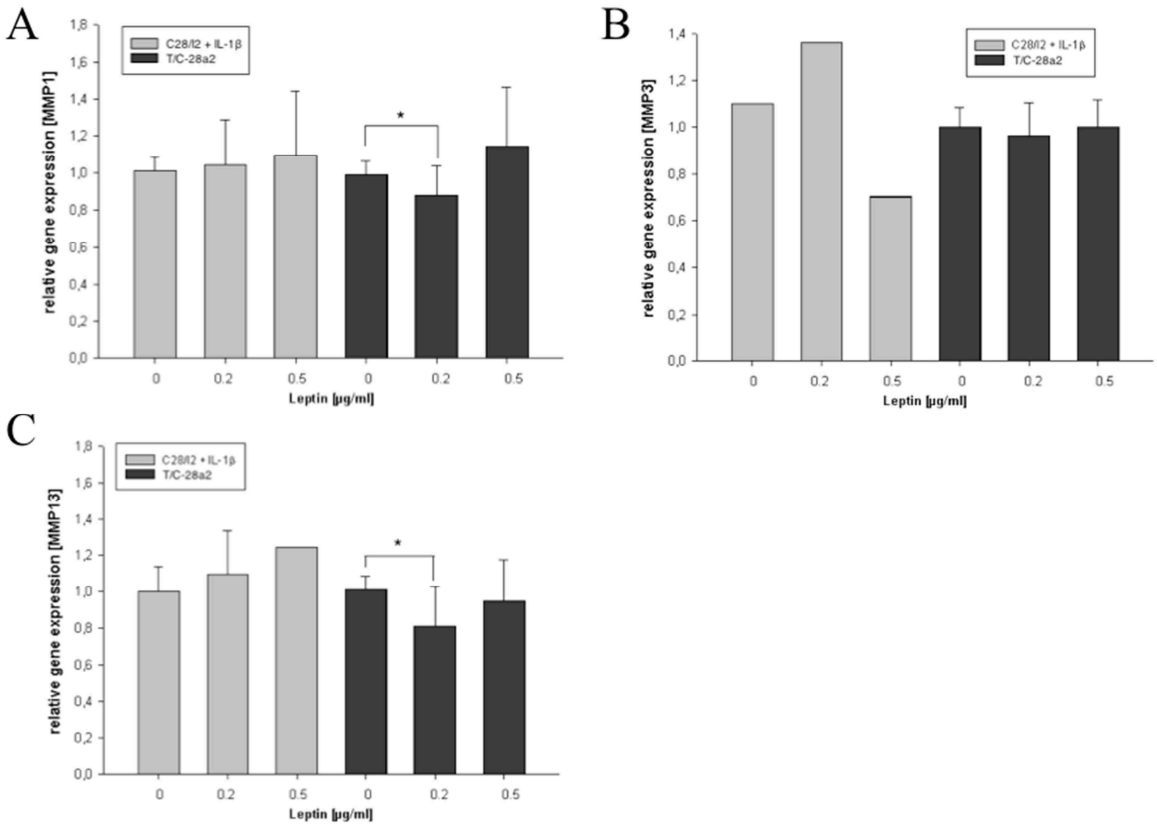

Figure 25. Gene expression of MMP-1, MMP-3 and MMP-13 after 48 h.
A: MMP-1 gene expression levels of C28/I2 and T/C-28a2 after 48 h of leptin [0.2 µg/ml; 0.5 µg/ml] treatment. **B:** MMP-3 gene expression levels of C28/I2 and T/C-28a2 after 48 h of leptin [0.2 µg/ml; 0.5 µg/ml] treatment. **C:** MMP-13 gene expression levels of C28/I2 and T/C-28a2 after 48 h of leptin [0.2 µg/ml; 0.5 µg/ml] treatment.

	C28/I2		
Leptin [µg/ml]	**Ctrl**	**0.2**	**0.5**
MMP-1	1.01 ± 0.07	1.04 ± 0.2	1.09 ± 0.3
MMP-3	1	1.36	0.70
MMP-13	1	1.1 ± 0.2	1.24

Table 11. MMP gene expression levels of C28/I2

T/C-28a2			
Leptin [µg/ml]	**Ctrl**	**0.2**	**0.5**
MMP-1	0.99± 0.07	0.85 ± 0.15 P= 0.0357	1.16 ± 0.3
MMP-3	1 ± 0.08	0.97 ± 0.1	1.003 ± 0.1
MMP-13	1.01 ± 0.07	0.81 ± 0.2 P= 0.0384	0.94 ± 0.2

Table 12. MMP gene expression levels of T/C-28a2

3.5.2 Collagen analysis

Collagen 1A1: The C28/I2 + IL-1β cell line indicated a significant decrease (p= 0.0141) of COL1A1 gene expression, when treated with leptin [0.2 µg/ml] and showed no effect compared to the non-treated control, when treated with leptin [0.5 µg/ml]. The expression of COL1A1 by the T/C-28a2 cells revealed no significant effect, but a declining tendency in connection with an increasing leptin concentration (Figure 26 A, Table 13 and 14).

Collagen 2A1: The C28/I2 + IL-1β cell line indicated a non-significant decrease of COL2A1 gene expression levels, when treated with leptin [0.2 µg/ml] and more decreasing when treated with leptin [0.5 µg/ml] compared to the control. Also the T/C-28a2 cell line showed a declining tendency of the COL2A1 gene expression, which depends on the increasing leptin concentration (Figure 26 B, Table 13 and 14).

Results are mean ± SD of 10 independent experiments carried out in triplicates.

C28/I2			
Leptin [µg/ml]	**Ctrl**	**0.2**	**0.5**
Col1A1	1.03 ± 0.07	0.83 ± 0.13 P= 0.0141	1.02 ± 0.18
Col2A1	1 ± 0.08	0.85 ± 0.09	0.94 ± 0.1

Table 13. Collagen gene expression levels of C28/I2

	T/C-28a2		
Leptin [µg/ml]	**Ctrl**	**0.2**	**0.5**
Col1A1	0.98 ± 0.08	0.98 ± 0.2	0.92 ± 0.19
Col2A1	1 ± 0.08	0.98 ± 0.91	0.89 ± 0.13

Table 14. Collagen gene expression levels of T/C-28a2

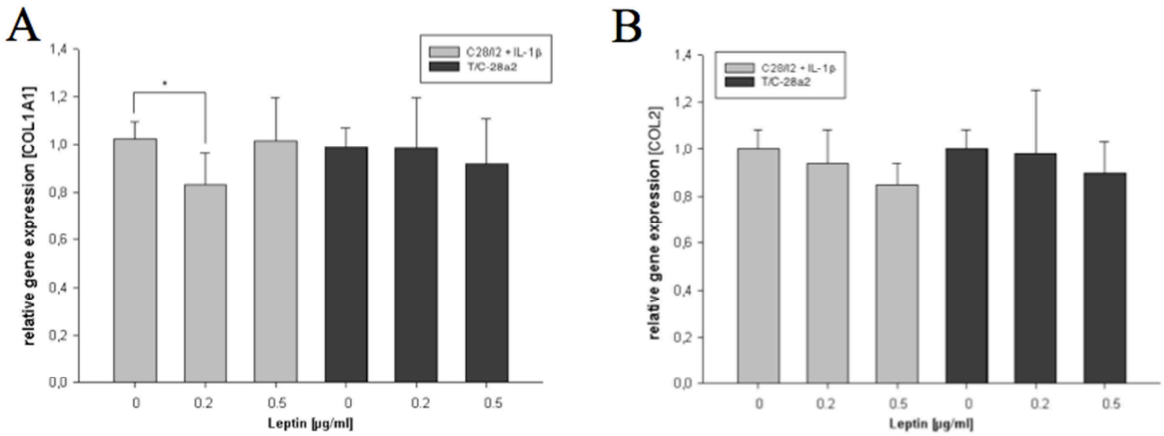

Figure 26. Gene expression levels of collagen 1A1 and collagen 2A1
A: COL1A1 gene expression analyses of C28/I2 and T/C-28a2 after 48 h. **B:** COL2A1 gene expression analyses of C28/I2 and T/C-28a2 after 48 h. Results are mean ± SD of 10 independent experiments carried out in triplicates.

3.6 SIRCOL™

In order to gain information about the newly synthesized collagen produced by C28/I2 ± IL-1β and T/C-28a2 after the treatment with leptin, the Sircol™ assay (n= 5), a colorimetric measurement method was used. Inflammatory conditions were set by using leptin in a concentration of 0.5 µg/ml. IL-1β was additionally used for defined parts of the C28/I2 seeding setup.

Results are mean ± standard deviation of 5 independent experiments done in duplicates (n = 5).

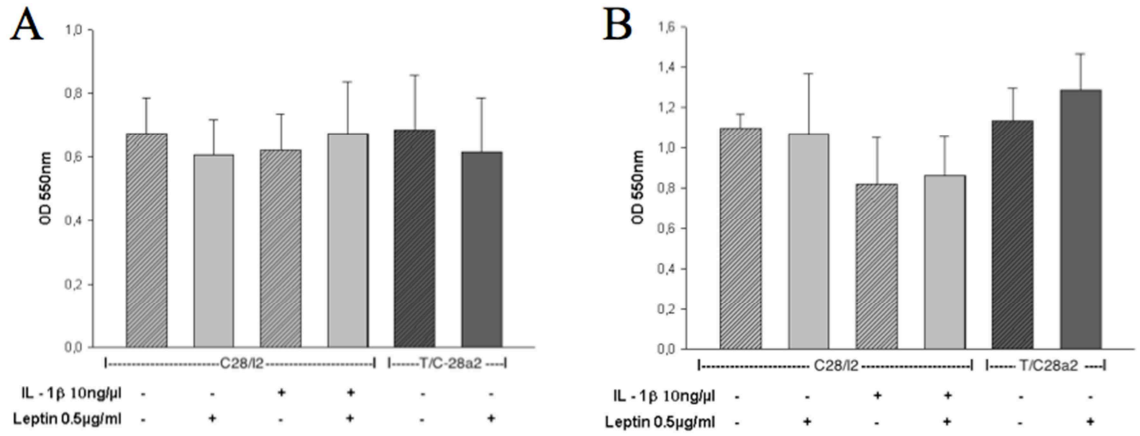

Figure 27: Colorimetric measurement of soluble collagen after Leptin treatment.
A) Spectrophotometrically measurement [550 nm] of newly synthesized collagen after 24 h and B) after 48h. Results are mean ± standard deviation of 5 independent experiments done in duplicates (n = 5).

C28/I2 showed a decreasing collagen production after 24 h, when treated with leptin [0.5 µg/ml] (0.67 ± 0.1) compared to the control (0.60 ± 0.1) (Figure 27 A). As well, a decrease after 48 h treatment could be observed (1.09 ± 0.1) towards the control group (1.06 ± 0.3) (Figure 27 B).

C28/I2 additionally treated with IL-1β and leptin [0.5 µg/ml] showed a non-significant increase of collagen after 24 h (0.62 ± 0.2) compared to the control group (0.67± 0.2) (Figure 27 A). Likewise after a time period of 48 h an increase of collagen production could be detected (0.82 ± 0.2) versus the control (0.86 ± 0.2), (Figure 27 B).

T/C-28a2 treated with leptin [0.5 µg/ml] indicated a decrease of collagen quantity after 24 h (0.68 ± 0.2) versus the non-treated cohort (0.61 ± 0.2), (Figure 27 A). Increasing change

in collagen quantity was analyzed after 48 h in treated T/C-28a2 (1.13 ± 0.1) towards the control (1.28 ± 0.2), (Figure 27 B).

3.7 BLYSCAN™

In order to analyze the quantity of sulfated glycosaminoglycan (sGAG) produced by C28/I2 ± IL-1β and TC28-a2 chondrocyte cell lines under inflammatory conditions the Blyscan™ assay was utilized. Inflammatory conditions were generated using leptin in a concentration of 0.5 µg/ml. IL-1β [10 ng/ml] was supplementary used for defined parts of the C28/I2 seeding scheme.

Results are mean ± standard deviation of five independent experiments done in duplicates (n= 5).

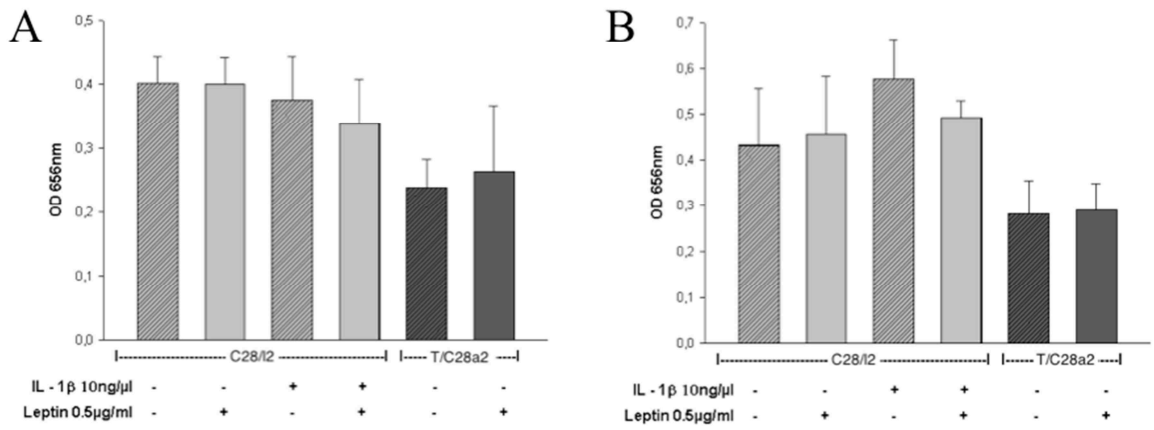

Figure 28: Colorimetric measurement of sGAG after Leptin treatment.
A) Spectrophotometrically measurement [550 nm] of newly synthesized collagen after 24 h and B) after 48 h. Results are mean ± standard deviation of 5 independent experiments done in duplicates (n = 5).

The sGAG production showed no change after 24 h in C28/I2 treated with leptin [0.5 µg/ml] (0.40 ± 0.04) towards the control group (0.40 ± 0.04), (Figure 28 A) and an increase after 48 h (0.43 ± 0.1) versus the control (0.45 ± 0.1), (Figure 28 B).

C28/I2 additionally treated with IL-1β [10 ng/µl] and leptin [0.5 µg/ml] showed no significant reduction of sGAG after 24 h (0.37± 0.1) compared to the control group (0.34 ± 0.1), (Figure 28 A) and also after a treatment period of 48 h a decrease of sGAG production was detected (0.57 ± 0.1) towards the control group (0.49 ± 0.03), (Figure 28 B).

T/C-28a2 treated with leptin [0.5 µg/ml] indicated an increase of the sGAG production past 24 h (0.23 ± 0.04) compared to the non-treated cells (0.26 ± 0.1), (Figure 28 A). No change in sGAG quantity was analyzed after 48 h in treated T/C-28a2 (0.28 ± 0.1) against the control group (0.28 ± 0.1), (Figure 28 B).

4 Discussion

Recent studies suggest that leptin is strongly linked to OA and obesity (58,78). Leptin has local effects on articular cartilage and there may be a relation between the grade of cartilage destruction and these specific local influences. Moreover a catabolic and pro-inflammatory role of leptin on cartilage metabolism is suggested, due to the production of Il-1β, MMP-9 and MMP-13 by chondrocytes after the treatment with leptin (53).

Experiments with leptin-signaling deficient mice showed that adiposity in absence of leptin signaling is insufficient to induce knee OA in female mice. These findings suggest a direct key role of leptin in the pathophysiology of OA (52).

Leptin exists in synovial fluids of OA-affected joints and leptin concentrations are correlated with the body mass index, which indicates an important role of leptin in the metabolism of human chondrocytes in connection with obesity. OA cartilage and osteophytes show a marked expression of leptin, whereas in healthy cartilage only a few chondrocytes produce leptin (47).

Interestingly leptin has also an anabolic role in human chondrocytes. Chondrocytes stimulated with leptin indicated an elevated synthesis of extracellular matrix (e.g. collagen) and an increased cell proliferation (60). In addition recent animal studies showed that leptin strongly stimulates anabolic functions of chondrocytes (47).

All these results point towards a complex and dualistic role of leptin regarding to human articular tissue, which brings up the question if leptin is the metabolic, non-mechanical link between OA and obesity?

The objective of this study was to gain information about the responsiveness of human chondrocyte cell lines C28/I2 and T/C-28a2 to elevated recombinant leptin levels. We designed our study by observing the cell growth behavior, the cell viability, and the gene expression changes of catabolic and anabolic factors (MMPs and collagen) and extracellular matrix changes (collagen and sGAG) after the treatment with recombinant leptin.

According to the findings of Cipolleta et al. which indicate a loss of sensitivity to exogenous stimulating factors, when cells are isolated from the extracellular matrix cf. cell culture conditions (79), we decided to use higher leptin concentrations [0.2 µg/ml; 0.5 µg/ml] than in synovial fluids of OA patients [1 up to 100 ng/ml] (46). By this we tried to walk the fine line between the loss of sensitivity and the findings of Pallu and colleagues, who suggest that chondrocytes under an obese condition may be refractory to further leptin stimulation due to their already existing exposition to highly elevated leptin levels (78).

Leptin possess a negative effect on the cell proliferation of human chondrocytes, especially with increasing leptin concentrations (53). The effect of leptin on cell proliferation in normal and OA-cultured chondrocytes was assessed. For one a stimulatory effect on cell proliferation in short-term cultures, for another a loss of this effect in long-term cultures was analyzed. With an increasing leptin concentration, the proliferation rate of chondrocytes decreased compared to the non-treated control group, suggesting a long- term detrimental effect of leptin on the cell viability. In our study we found C28/I2 and T/C-28a2 to be almost unresponsive to leptin [0.001 µg/ml; 0.01 µg/ml; 0.1 µg/ml; 0.5 µg/ml; 1.0 µg/ml] over a time period of 24 h and 48 h, showing no significant negative effect on the cell viability (Figure 22). Further studies are needed to examine, what may be the reasons for these contrary findings e.g. a slightly difference in long-term culture conditions or the source of the adipokine.

Previous experiments from other researchers with related subjects were performed with a cell culture medium without foetal bovine serum (FBS). Especially when it comes to the plating of the cells (53,78,80), they used a serum derived cell culture medium. Our real-time growth measurement showed that the human chondrocyte cell lines C28/I2 and T/C-28a2 will not grow regularly without FBS as shown in Figure 21. As a consequence to these findings we used a setup, whereby cells were plated with FBS. These divergences may occur due to many factors e.g. the tissue examined (immortalized cell lines versus cultured primary chondrocytes).

It has to be investigated which influences the essential addition of FBS (Figure 21.) has on the used colorimetric assays or if there are interactions between FBS and the recombinant leptin, which affect the results.

We used the immortalized chondrocyte cell lines C28/I2 and T/C-28a2, despite not being an entire ideal study design concerning possible occurring problems like the loss of sensitivity of chondrocytes towards exogenous stimuli when isolated from ECM or the suggested refractory state of the chondrocytes in a highly inflammatory setting or the essential addition of FBS required by these cell lines. Since primary chondrocytes are expensive and not available to the extent needed, especially for experiments performed to study the gene expression levels, which need high levels of reproducibility and therefore a high quantity of cells.

Leptin enhances the production of the cartilage degrading metalloproteinases (MMP) MMP-1, MMP-3 and MMP-13 in human OA cartilage. Furthermore a significant positive correlation of leptin levels in synovial fluids and MMP-1 and MMP-3 levels was detected (49). The matrix degrading MMP-1, MMP-9 and MMP-13 were also subject in other studies and were confirmed to have higher expression levels in chondrocytes treated with leptin compared to a control cohort (53,78,80).

We were able to confirm a slight dosage-dependent responsiveness of C28/I2 cells regarding the up regulation of MMP-1 and MMP-13 (Figure 25). Interestingly we could not confirm an increase of these catabolic genes in the T/C-28a2 cell line, against expectations we detected a significant decrease of MMP-1 and MMP-13 expressed by T/C-28a2 cells (Figure 25) when treated with leptin in the lower dosage. Furthermore in our study an increase of MMP-9 expression remains undetectable (data not shown). MMP-9 was shown to be up regulated in chondrocytes as well as MMP-1, MMP-3 and MMP-13 after the incubation with leptin (53,58).

A biphasic effect of leptin in primary human articular chondrocytes with an effect optimum between 0.1 to 100 ng/ml leptin was observed (60). The reduced effect of leptin at a higher leptin concentration may occur due to a possible negative feedback-loop.
In 2016 the group around Koskinen observed, that on the one hand MMP-1, MMP-3 and MMP-13 expressions were higher in cartilage tissue with a low level of suppressor of cytokine signaling-3 (SOCS-3) and on the other hand metalloproteinase expressions were lower in cartilage tissues with a high level of SOCS- 3 (81). These results demonstrate a regulation of leptin-induced responses in cartilage, equivalent to a negative feedback- loop.

Further studies have to be performed, in order to gain information about if these regulation mechanisms are also valid for immortalized chondrocyte cell lines and if these regulations may be a possible answer to the contrary findings of our study.

Moreover we investigated the gene expression levels of collagen 1A1 (Col1A1) and collagen 2 (Col2A1) in chondrocyte cell lines via RT-qPCR after the treatment with leptin (Figure 26). The chondrocyte cell lines showed a minor dosage-dependent decrease of expression levels in both genes, in contrast to the findings of other groups, that chondrocytes treated with leptin responded with an up regulation of collagen 2A1 (58,78). Related to Col1A1 previous data only exist for type I procollagen peptides, which were detected to be scattered up regulated in primary chondrocytes after a treatment with leptin suggesting a consecutive collagen 1 up regulation (82). Interestingly our results showed a significant decrease of collagen 1A1 after the treatment with the menial leptin concentration.

Col2A1 has a critical role as cartilage-specific regulator of cartilage catabolism and may also be a contributor in the pathogenesis of OA (83). Furthermore Col2A1 plays a protective compensatory role in normal cartilage treated with leptin (84) and collagen-dependent cartilage degration is an important factor in physiological cartilage turnover (58). These findings make us expect, that leptin has a complex role in catabolic cartilage mechanisms.

Additionally we analyzed the collagen expression on a protein level via colorimetric assay (Figure 27). We found collagen to be slightly up regulated in the leptin+IL-1β setup (C28/I2), whereas C28/I2 without IL-1β showed a slight decrease of collagen, which may support the idea of a compensatory protective mechanism (58). Our findings concerning the T/C-28a2 cell lines appeared to be inconsistent and therefore not definite to assess.
Sulfated glycosaminoglycan (sGAG) as a major component of the extracellular matrix was analyzed as well via colorimetric assay (Figure 28). We could not detect significant changes in the sGAG expression in protein levels but a declining leptin+IL-1β induced tendency of the expression of sGAG. As well as occurred in our collagen ECM analyzes the sGAG findings were also not decisive enough to be evaluate, due to their inconsistency.

Our study provides interesting insights in the responsiveness of human chondrocyte cell lines C28/I2 and T/C-28a2 and therefore interesting information about the pathogenesis of OA and the relation between obesity and OA.
In virtue of many influencing factors it has to be discussed for future studies e.g. which chondrocyte cell types to use best (immortalized cell lines versus primary chondrocyte) or which source of adipokine is suitable (recombinant leptin versus human leptin mixtures) to take a step towards physiological *in vitro* studies.

However, further studies are required to establish a physiological *in vitro* study design and to elucidate the complex mechanisms of leptin in obese individuals who are afflicted with OA, to find new targets in the therapy of OA.

5 References

1. Berenbaum F. Osteoarthritis as an inflammatory disease (osteoarthritis is not osteoarthrosis!). Osteoarthritis Cartilage. 2013 Jan 1;21(1):16–21.

2. Kraan PM van der. Osteoarthritis year 2012 in review: biology. Osteoarthritis Cartilage. 2012 Dec 1;20(12):1447–50.

3. Moyer RF, Hunter DJ. Osteoarthritis in 2014: Changing how we define and treat patients with OA. Nat Rev Rheumatol. 2015 Feb;11(2):65–6.

4. Kellgren JH, Lawrence JS. Radiological Assessment of Osteo-Arthrosis. Ann Rheum Dis. 1957 Dec;16(4):494–502.

5. Hunter DJ, Arden N, Conaghan PG, Eckstein F, Gold G, Grainger A, et al. Definition of osteoarthritis on MRI: results of a Delphi exercise. Osteoarthritis Cartilage. 2011 Aug;19(8):963–9.

6. Guermazi A, Niu J, Hayashi D, Roemer FW, Englund M, Neogi T, et al. Prevalence of abnormalities in knees detected by MRI in adults without knee osteoarthritis: population based observational study (Framingham Osteoarthritis Study). The BMJ [Internet]. 2012 Aug 29 [cited 2016 May 4];345. Available from: http://www.ncbi.nlm.nih.gov/pmc/articles/PMC3430365/

7. Peterfy CG, Guermazi A, Zaim S, Tirman PFJ, Miaux Y, White D, et al. Whole-Organ Magnetic Resonance Imaging Score (WORMS) of the knee in osteoarthritis. Osteoarthritis Cartilage. 2004 Mar 1;12(3):177–90.

8. Hunter DJ, Guermazi A, Lo GH, Grainger AJ, Conaghan PG, Boudreau RM, et al. Evolution of semi-quantitative whole joint assessment of knee OA: MOAKS (MRI Osteoarthritis Knee Score). Osteoarthritis Cartilage. 2011 Aug 1;19(8):990–1002.

9. Loeser RF, Goldring SR, Scanzello CR, Goldring MB. Osteoarthritis: A disease of the joint as an organ. Arthritis Rheum. 2012 Jun 1;64(6):1697–707.

10. Lozano R, Naghavi M, Foreman K, Lim S, Shibuya K, Aboyans V, et al. Global and regional mortality from 235 causes of death for 20 age groups in 1990 and 2010: a systematic analysis for the Global Burden of Disease Study 2010. The Lancet. 2012 Dec;380(9859):2095–128.

11. WHO | Chronic rheumatic conditions [Internet]. WHO. [cited 2016 May 4]. Available from: http://www.who.int/chp/topics/rheumatic/en/

12. Marshall DA, Vanderby S, Barnabe C, MacDonald KV, Maxwell C, Mosher D, et

al. Estimating the Burden of Osteoarthritis to Plan for the Future: Using Administrative Health Data to Estimate OA Rates. Arthritis Care Res. 2015 Oct;67(10):1379–86.

13. Lawrence RC, Felson DT, Helmick CG, Arnold LM, Choi H, Deyo RA, et al. Estimates of the prevalence of arthritis and other rheumatic conditions in the United States: Part II. Arthritis Rheum. 2008 Jan 1;58(1):26–35.

14. Srikanth VK, Fryer JL, Zhai G, Winzenberg TM, Hosmer D, Jones G. A meta-analysis of sex differences prevalence, incidence and severity of osteoarthritis. Osteoarthritis Cartilage. 2005 Sep;13(9):769–81.

15. Spector TD, MacGregor AJ. Risk factors for osteoarthritis: genetics1. Osteoarthritis Cartilage. 2004 Jan 1;12:39–44.

16. Felson DT, Lawrence RC, Dieppe PA, Hirsch R, Helmick CG, Jordan JM, et al. Osteoarthritis: New Insights. Part 1: The Disease and Its Risk Factors. Ann Intern Med. 2000 Oct 17;133(8):635–46.

17. Chapman K, Takahashi A, Meulenbelt I, Watson C, Rodriguez-Lopez J, Egli R, et al. A meta-analysis of European and Asian cohorts reveals a global role of a functional SNP in the 5′ UTR of GDF5 with osteoarthritis susceptibility. Hum Mol Genet. 2008 May 15;17(10):1497–504.

18. Palotie A, Ott J, Elima K, Cheah K, Väisänen P, Ryhänen L, et al. PREDISPOSITION TO FAMILIAL OSTEOARTHROSIS LINKED TO TYPE II COLLAGEN GENE. The Lancet. 1989 Apr;333(8644):924–7.

19. Evangelou E, Valdes AM, Kerkhof HJ., Styrkarsdottir U, Zhu Y, Meulenbelt I, et al. Meta-analysis of genome-wide association studies confirms a susceptibility locus for knee osteoarthritis on chromosome 7q22. Ann Rheum Dis. 2011 Feb;70(2):349–55.

20. Day-Williams AG, Southam L, Panoutsopoulou K, Rayner NW, Esko T, Estrada K, et al. A Variant in MCF2L Is Associated with Osteoarthritis. Am J Hum Genet. 2011 Sep 9;89(3):446–50.

21. Valdes AM, Evangelou E, Kerkhof HJM, Tamm A, Doherty SA, Kisand K, et al. The GDF5 rs143383 polymorphism is associated with osteoarthritis of the knee with genome-wide statistical significance. Ann Rheum Dis. 2011 May;70(5):873–5.

22. Messier SP, Legault C, Mihalko S, Miller GD, Loeser RF, DeVita P, et al. The Intensive Diet and Exercise for Arthritis (IDEA) trial: design and rationale. BMC Musculoskelet Disord. 2009 Jul 28;10:93.

23. Hadler NM, Gillings DB, Imbus HR, Levitin PM, Makuc D, Utsinger PD, et al.

Hand structure and function in an industrial setting. Arthritis Rheum. 1978 Mar 1;21(2):210–20.

24. Hunter DJ, Eckstein F. Exercise and osteoarthritis. J Anat. 2009 Feb 1;214(2):197–207.

25. Slauterbeck JR, Kousa P, Clifton BC, Naud S, Tourville TW, Johnson RJ, et al. Geographic Mapping of Meniscus and Cartilage Lesions Associated with Anterior Cruciate Ligament Injuries. J Bone Jt Surg Am. 2009 Sep 1;91(9):2094–103.

26. Lane NE, Lin P, Christiansen L, Gore LR, Williams EN, Hochberg MC, et al. Association of mild acetabular dysplasia with an increased risk of incident hip osteoarthritis in elderly white women: The study of osteoporotic fractures. Arthritis Rheum. 2000 Feb 1;43(2):400–4.

27. Zhuo Q, Yang W, Chen J, Wang Y. Metabolic syndrome meets osteoarthritis. Nat Rev Rheumatol. 2012 Dec;8(12):729–37.

28. WHO | Obesity and overweight [Internet]. WHO. [cited 2016 May 17]. Available from: http://www.who.int/mediacentre/factsheets/fs311/en/

29. Fermor B, Weinberg JB, Pisetsky DS, Misukonis MA, Fink C, Guilak F. Induction of cyclooxygenase-2 by mechanical stress through a nitric oxide-regulated pathway. Osteoarthr Cartil OARS Osteoarthr Res Soc. 2002 Oct;10(10):792–8.

30. Fujisawa T, Hattori T, Takahashi K, Kuboki T, Yamashita A, Takigawa M. Cyclic mechanical stress induces extracellular matrix degradation in cultured chondrocytes via gene expression of matrix metalloproteinases and interleukin-1. J Biochem (Tokyo). 1999 May;125(5):966–75.

31. Honda K, Ohno S, Tanimoto K, Ijuin C, Tanaka N, Doi T, et al. The effects of high magnitude cyclic tensile load on cartilage matrix metabolism in cultured chondrocytes. Eur J Cell Biol. 2000 Sep;79(9):601–9.

32. Lin PM, Chen C-TC, Torzilli PA. Increased stromelysin-1 (MMP-3), proteoglycan degradation (3B3- and 7D4) and collagen damage in cyclically load-injured articular cartilage. Osteoarthr Cartil OARS Osteoarthr Res Soc. 2004 Jun;12(6):485–96.

33. Thijssen E, Caam A van, Kraan PM van der. Obesity and osteoarthritis, more than just wear and tear: pivotal roles for inflamed adipose tissue and dyslipidaemia in obesity-induced osteoarthritis. Rheumatology. 2015 Apr 1;54(4):588–600.

34. Cicuttini FM, Baker JR, Spector TD. The association of obesity with osteoarthritis of the hand and knee in women: a twin study. J Rheumatol. 1996 Jul;23(7):1221–6.

35. Gregor MF, Hotamisligil GS. Inflammatory mechanisms in obesity. Annu Rev Immunol. 2011;29:415–45.

36. Klop B, Elte JWF, Castro Cabezas M. Dyslipidemia in Obesity: Mechanisms and Potential Targets. Nutrients. 2013 Apr 12;5(4):1218–40.

37. Davies-Tuck ML, Hanna F, Davis SR, Bell RJ, Davison SL, Wluka AE, et al. Total cholesterol and triglycerides are associated with the development of new bone marrow lesions in asymptomatic middle-aged women - a prospective cohort study. Arthritis Res Ther. 2009;11(6):R181.

38. Nguyen MTA, Favelyukis S, Nguyen A-K, Reichart D, Scott PA, Jenn A, et al. A Subpopulation of Macrophages Infiltrates Hypertrophic Adipose Tissue and Is Activated by Free Fatty Acids via Toll-like Receptors 2 and 4 and JNK-dependent Pathways. J Biol Chem. 2007 Nov 30;282(48):35279–92.

39. Triantaphyllidou I-E, Kalyvioti E, Karavia E, Lilis I, Kypreos KE, Papachristou DJ. Perturbations in the HDL metabolic pathway predispose to the development of osteoarthritis in mice following long-term exposure to western-type diet. Osteoarthritis Cartilage. 2013 Feb 1;21(2):322–30.

40. Akagi M, Kanata S, Mori S, Itabe H, Sawamura T, Hamanishi C. Possible involvement of the oxidized low-density lipoprotein/lectin-like oxidized low-density lipoprotein receptor-1 system in pathogenesis and progression of human osteoarthritis. Osteoarthritis Cartilage. 2007 Mar 1;15(3):281–90.

41. Zhang Y, Proenca R, Maffei M, Barone M, Leopold L, Friedman JM. Positional cloning of the mouse obese gene and its human homologue. Nature. 1994 Dec 1;372(6505):425–32.

42. Barr VA, Lane K, Taylor SI. Subcellular Localization and Internalization of the Four Human Leptin Receptor Isoforms. J Biol Chem. 1999 Jul 23;274(30):21416–24.

43. Frühbeck G. Intracellular signalling pathways activated by leptin. Biochem J. 2006 Jan 1;393(1):7–20.

44. Lee G-H, Proenca R, Montez JM, Carroll KM, Darvishzadeh JG, Lee JI, et al. Abnormal splicing of the leptin receptor in diabetic mice. Nature. 1996 Feb 15;379(6566):632–5.

45. Tartaglia LA. The Leptin Receptor. J Biol Chem. 1997 Mar 7;272(10):6093–6.

46. Presle N, Pottie P, Dumond H, Guillaume C, Lapicque F, Pallu S, et al. Differential distribution of adipokines between serum and synovial fluid in patients with osteoarthritis.

Contribution of joint tissues to their articular production. Osteoarthritis Cartilage. 2006 Jul;14(7):690–5.

47. Dumond H, Presle N, Terlain B, Mainard D, Loeuille D, Netter P, et al. Evidence for a key role of leptin in osteoarthritis. Arthritis Rheum. 2003 Nov 1;48(11):3118–29.

48. Karvonen-Gutierrez CA, Harlow SD, Mancuso P, Jacobson J, Mendes de Leon CF, Nan B. Association of Leptin Levels With Radiographic Knee Osteoarthritis Among a Cohort of Midlife Women: Serum Leptin Levels and Prevalent and Incident Radiographic Knee OA. Arthritis Care Res. 2013 Jun;65(6):936–44.

49. Koskinen A, Vuolteenaho K, Nieminen R, Moilanen T, Moilanen E. Leptin enhances MMP-1, MMP-3 and MMP-13 production in human osteoarthritic cartilage and correlates with MMP-1 and MMP-3 in synovial fluid from OA patients. Clin Exp Rheumatol. 2011 Feb;29(1):57–64.

50. Ku JH, Lee CK, Joo BS, An BM, Choi SH, Wang TH, et al. Correlation of synovial fluid leptin concentrations with the severity of osteoarthritis. Clin Rheumatol. 2009 Dec;28(12):1431–5.

51. Lübbeke A, Finckh A, Puskas GJ, Suva D, Lädermann A, Bas S, et al. Do synovial leptin levels correlate with pain in end stage arthritis? Int Orthop. 2013 Oct;37(10):2071–9.

52. Griffin TM, Huebner JL, Kraus VB, Guilak F. Extreme obesity due to impaired leptin signaling in mice does not cause knee osteoarthritis. Arthritis Rheum. 2009 Oct;60(10):2935–44.

53. Simopoulou T, Malizos KN, Iliopoulos D, Stefanou N, Papatheodorou L, Ioannou M, et al. Differential expression of leptin and leptin's receptor isoform (Ob-Rb) mRNA between advanced and minimally affected osteoarthritic cartilage; effect on cartilage metabolism. Osteoarthritis Cartilage. 2007 Aug;15(8):872–83.

54. Otero M, Reino JJG, Gualillo O. Synergistic induction of nitric oxide synthase type II: In vitro effect of leptin and interferon-? in human chondrocytes and ATDC5 chondrogenic cells. Arthritis Rheum. 2003 Feb;48(2):404–9.

55. Otero M, Lago R, Lago F, Reino JJG, Gualillo O. Signalling pathway involved in nitric oxide synthase type II activation in chondrocytes: synergistic effect of leptin with interleukin-1. Arthritis Res Ther. 2005;7(3):R581–91.

56. Gomez R, Scotece M, Conde J, Gomez-Reino JJ, Lago F, Gualillo O. Adiponectin and leptin increase IL-8 production in human chondrocytes. Ann Rheum Dis. 2011 Nov 1;70(11):2052–4.

57. Conde J, Scotece M, López V, Gómez R, Lago F, Pino J, et al. Adiponectin and Leptin Induce VCAM-1 Expression in Human and Murine Chondrocytes. Neves NM, editor. PLoS ONE. 2012 Dec 19;7(12):e52533.

58. Bao J, Chen W, Feng J, Hu P, Shi Z, Wu L. Leptin plays a catabolic role on articular cartilage. Mol Biol Rep. 2010 Oct;37(7):3265–72.

59. Iliopoulos D, Malizos KN, Tsezou A. Epigenetic regulation of leptin affects MMP-13 expression in osteoarthritic chondrocytes: possible molecular target for osteoarthritis therapeutic intervention. Ann Rheum Dis. 2007 Dec 1;66(12):1616–21.

60. Figenschau Y, Knutsen G, Shahazeydi S, Johansen O, Sveinbjörnsson B. Human Articular Chondrocytes Express Functional Leptin Receptors. Biochem Biophys Res Commun. 2001 Sep 14;287(1):190–7.

61. Scotece M, Mobasheri A. Leptin in osteoarthritis: Focus on articular cartilage and chondrocytes. Life Sci. 2015 Nov 1;140:75–8.

62. Emery's elements of medical genetics / Peter Turnpenny, Sian Ellard. - Version details [Internet]. Trove. [cited 2016 Aug 16]. Available from: http://trove.nla.gov.au/version/45537409

63. Hohoff C, Brinkmann B. Human identity testing with PCR-based systems. Mol Biotechnol. 13(2):123–36.

64. iCELLigence - ACEA Biosciences Inc. [Internet]. [cited 2016 Oct 24]. Available from: https://aceabio.com/product/icelligence/

65. CellTiter 96® AQueous One Solution Cell Proliferation Assay System Protocol [Internet]. [cited 2016 Oct 24]. Available from: https://www.promega.de/resources/protocols/technical-bulletins/0/celltiter-96-aqueous-one-solution-cell-proliferation-assay-system-protocol/

66. Bartlett JS, Stirling D. A Short History of the Polymerase Chain Reaction. In: Bartlett JS, Stirling D, editors. PCR Protocols [Internet]. Humana Press; 2003 [cited 2016 Aug 13]. p. 3–6. (Methods in Molecular Biology™). Available from: http://dx.doi.org/10.1385/1-59259-384-4%3A3

67. Polymerase Chain Reaction (PCR) [Internet]. [cited 2016 Oct 24]. Available from: https://www.ncbi.nlm.nih.gov/probe/docs/techpcr/

68. Real-Time Quantitative Reverse Transcription PCR [Internet]. [cited 2016 Oct 24]. Available from: https://www.ncbi.nlm.nih.gov/probe/docs/techqpcr/

69. Real-Time PCR Handbook | Thermo Fisher Scientific [Internet]. [cited 2016 Oct

24]. Available from: https://www.thermofisher.com/de/de/home/life-science/pcr/real-time-pcr/qpcr-education/real-time-pcr-handbook.html

70. Bustin SA, Benes V, Garson JA, Hellemans J, Huggett J, Kubista M, et al. The MIQE Guidelines: Minimum Information for Publication of Quantitative Real-Time PCR Experiments. Clin Chem. 2009 Apr 1;55(4):611–22.

71. Bustin SA, Beaulieu J-F, Huggett J, Jaggi R, Kibenge FS, Olsvik PA, et al. MIQE précis: Practical implementation of minimum standard guidelines for fluorescence-based quantitative real-time PCR experiments. BMC Mol Biol. 2010 Sep 21;11:74.

72. RNA Isolation Kit: RNeasy Mini Kit - QIAGEN Online Shop [Internet]. [cited 2016 Oct 24]. Available from: https://www.qiagen.com/no/shop/epigenetics/rneasy-mini-kit/#productdetails

73. RNA quality control [Internet]. [cited 2016 Oct 24]. Available from: http://biomedicalgenomics.org/RNA_quality_control.html

74. Dyes, probes and chemistries in real-time PCR detection [Internet]. [cited 2016 Oct 24]. Available from: http://dyes.gene-quantification.info/

75. Vandesompele J, De Preter K, Pattyn F, Poppe B, Van Roy N, De Paepe A, et al. Accurate normalization of real-time quantitative RT-PCR data by geometric averaging of multiple internal control genes. Genome Biol. 2002 Jun 18;3(7):RESEARCH0034.

76. Sircol™ Soluble Collagen Assay [Internet]. extracellular matrix assays for use with mammalian cells, tissues and fluids. [cited 2016 Aug 6]. Available from: http://www.biocolor.co.uk/product/sircol-soluble-collagen-assay/

77. Blyscan™ Glycosaminoglycan Assay [Internet]. extracellular matrix assays for use with mammalian cells, tissues and fluids. [cited 2016 Aug 6]. Available from: http://www.biocolor.co.uk/product/blyscan-glycosaminoglycan-assay/

78. Pallu S, Francin P-J, Guillaume C, Gegout-Pottie P, Netter P, Mainard D, et al. Obesity affects the chondrocyte responsiveness to leptin in patients with osteoarthritis. Arthritis Res Ther. 2010;12(3):R112.

79. Cipolletta C, Jouzeau J-Y, Gegout-Pottie P, Presle N, Bordji K, Netter P, et al. Modulation of IL-1-induced cartilage injury by NO synthase inhibitors: a comparative study with rat chondrocytes and cartilage entities. Br J Pharmacol. 1998 Aug;124(8):1719–27.

80. Hui W, Litherland GJ, Elias MS, Kitson GI, Cawston TE, Rowan AD, et al. Leptin produced by joint white adipose tissue induces cartilage degradation via upregulation and

activation of matrix metalloproteinases. Ann Rheum Dis. 2012 Mar 1;71(3):455–62.

81. Koskinen-Kolasa A, Vuolteenaho K, Korhonen R, Moilanen T, Moilanen E. Catabolic and proinflammatory effects of leptin in chondrocytes are regulated by suppressor of cytokine signaling-3. Arthritis Res Ther [Internet]. 2016 Dec [cited 2016 Oct 16];18(1). Available from: http://arthritis-research.biomedcentral.com/articles/10.1186/s13075-016-1112-0

82. Berry PA, Jones SW, Cicuttini FM, Wluka AE, Maciewicz RA. Temporal relationship between serum adipokines, biomarkers of bone and cartilage turnover, and cartilage volume loss in a population with clinical knee osteoarthritis. Arthritis Rheum. 2011 Mar;63(3):700–7.

83. Klatt AR, Paul-Klausch B, Klinger G, Kühn G, Renno JH, Banerjee M, et al. A critical role for collagen II in cartilage matrix degradation: Collagen II induces pro-inflammatory cytokines and MMPs in primary human chondrocytes. J Orthop Res. 2009 Jan;27(1):65–70.

84. Gordeladze JO, Drevon CA, Syversen U, Reseland JE. Leptin stimulates human osteoblastic cell proliferation, de novo collagen synthesis, and mineralization: Impact on differentiation markers, apoptosis, and osteoclastic signaling. J Cell Biochem. 2002;85(4):825–36.